Table 1 ARBSs identified in the encyclopedia of DNA element (ENCODE) regions by ChIP-chip experiments

ARBS no.	*ENCODE region*	*Chromosome*	*Start*	*Stop*	*Closest gene*	*Distance from TSS (bp)*[a]	*Position*
1	ENr131	2	234 433 433	234 433 623	UGT1A1	−17 390	5′ upstream
2	ENr334	6	41 823 411	41 823 433	PGC	−323	5′ upstream
3	ENm010	7	26 807 344	26 807 566	SCAP2	−129 874	5′ upstream
4	ENm013	7	89 501 530	89 501 614	STEAP2	+15 922	intron 3
5	ENm013	7	89 980 335	89 980 369	PFTK1	−3010	5′ upstream
6	ENm001	7	115 551 316	115 551 473	TES	+106 864	3′ downstream
7	ENm001	7	116 022 567	116 022 922	MET	+116 336	intron 17
8	ENr233	15	41 640 443	41 640 980	KIAA0377	+23 671	intron 27
9	ENr233	15	41 739 974	41 740 495	CATSPER2	−11 904	5′ upstream
10	ENr213	18	23 990 311	23 990 793	CDH2	+20 637	intron1

Abbreviations: ARBs, androgen receptor-binding sites; TSS, transcriptional start site. [a]Distance from the TSS of the closet RefSeq gene to the corresponding ARBS based on the genomic position published in NCBI Build 35.

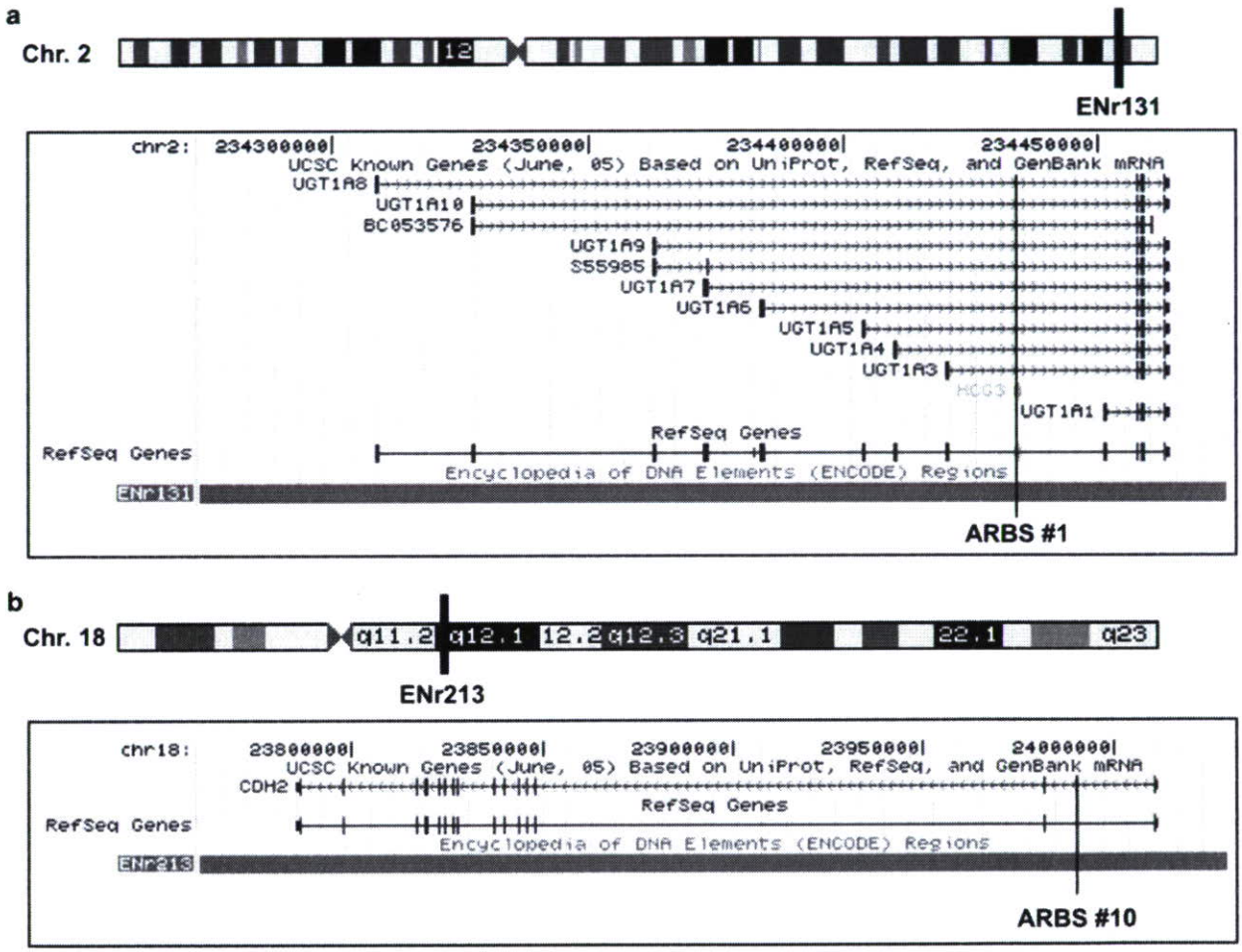

Figure 1 Identification of *in vivo* ARBSs in LNCaP cells on the encyclopedia of DNA elements (ENCODE) array by ChIP-chip analysis. (**a**) An expanded view of the UGT1A locus on the ENCODE region ENr131 from chromosome 2q37 is shown in its genuine 5′–3′ orientation. ARBS no. 1 is located on the 5′ upstream region of UGT1A1, or on intron 1 of other UGT1A isoforms. (**b**) An expanded view of the CDH2 on the ENCODE region ENr213 from chromosome 18q11.2 is shown in its genuine 3′–5′ orientation. ARBS no. 10 is located on intron 1 of CDH2.

confirmed that >10-fold enrichment of R1881-dependent AR binding was shown in the all regions involved in the defined 10 ARBSs, targeting the identified ARE sequences (Figure 2). Thus, with the cutoff value 1e-5, we validated that our ChIP-chip results did not include false positives.

Identification of androgen target genes adjacent to AR-binding sites

To identify novel androgen target genes by using ChIP-chip data, we examined the alteration of gene expression closest to the ARBSs in LNCaP cells in response to R1881 (Figure 3). Eight of 10 genes adjacent to the

Table 2 ARE sequences identified in the ARBSs detected by ENCODE chip

ARBS no.	*Gene*	*Distance from TSS (bp)*	*Position*	*Chromosome*	*Genomic location*	*Strand*	*ARE sequence*
1	UGT1A1	−17422	5′	2	234433576	+1	TGAACAttcTGTCCT
2	PGC	−399	5′	6	41823498	+1	GGAACAaatAGTTCT
3	SCAP2	−130006	5′	7	26807587	−1	AGAACCccaGGACCC
4	STEAP2	15941	INTRON 3	7	89501592	+1	GGAAAGaatTGTTCT
5	PFTK1	−2978	5′	7	89980382	−1	AGTAAGaagAGTTGC*
		−2947	5′	7	89980415	−1	ACAGCActcAGTACT*
6	TES	+106870	3′	7	115551402	+1	AAAACActcAGTTGC*
7	MET	+116298	INTRON 17	7	116022708	+1	TGCACAgtgTTTTAC*
8	KIAA0377	+27774	INTRON 27	15	41640739	−1	TAACCAtccTGTACC
9	CATSPER2	−11955	5′	15	41740290	−1	TAACCAtccTGTACC
10	CDH2	+20827	INTRON1	18	23990362	−1	GGTACAgaaTGTCAC
		+20805	INTRON1	18	23990384	−1	GGTACAgaaTGTCAC
		+20761	INTRON1	18	23990428	−1	GGTACAgcaTGTCAC
		+20739	INTRON1	18	23990450	−1	GGTACAgaaTGTCAC
		+20695	INTRON1	18	23990494	−1	GGTACAgcaTGTCAC
		+20673	INTRON1	18	23990516	−1	GGTACAgcaTGTCAC
		+20651	INTRON1	18	23990538	−1	GGTACAgaaTGTCAC
		+20629	INTRON1	18	23990560	−1	GGTACAgcaTGTCAC
		+20607	INTRON1	18	23990582	−1	GGTACAgcaTGTCAC
		+20541	INTRON1	18	23990648	−1	GGTACAgcaTGTCAC
		+20519	INTRON1	18	23990670	−1	GGTACAgcaTGTCAC
		+20651	INTRON1	18	23990538	−1	GGTACAgaaTGTCAC
		+20453	INTRON1	18	23990736	−1	GGTACAgaaTGTCAC

ARE sequences were primarily determined by a position-weighted matrix method TRANSFAC with the matrix conservation >75% (Matys *et al.*, 2003). If no ARE was predicted by the first criteria, alternative ARE sequences (indicated as *) were determined by a sequence analysis utility of JASPER with the relative profile score threshold >70% (Sandelin *et al.*, 2004). Genomic location of ARE sequence indicates the position of the center base.

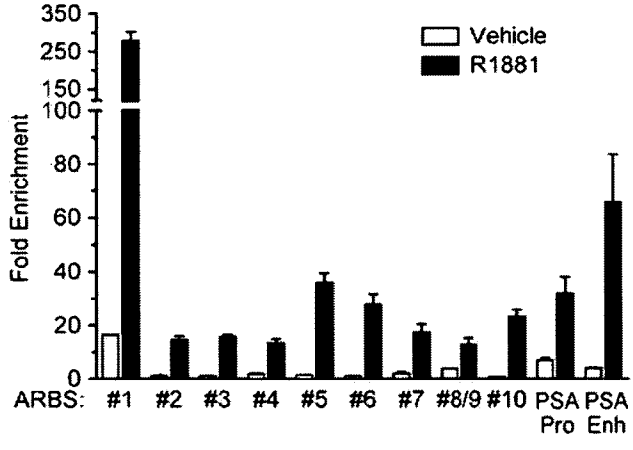

Figure 2 Validation of androgen-dependent AR enrichment by quantitative ChIP analysis on the identified ChIP-chip ARBSs in LNCaP cells. Hormone-deprivated cells were stimulated with R1881 (10 nM) or vehicle (0.1% ethanol) for 24 h. Cross-linked samples were immunoprecipitated with anti-AR antibody. The precipitated DNA fragments were subjected to qPCR. PCR primer sets were designed to include ARE sequences on individual ARBSs no. 1–no. 10. PCR products including ARBSs no. 8 and no. 9 were not distinguishable, as ARBSs no. 8 and no. 9 are located in genome duplication regions from the same origin. PSA promoter (PSA Pro) and enhancer (PSA Enh) regions including ARE sequences were used as positive controls. Data are fold enrichment compared with individual input non-enriched DNA (mean ± s.d., $n=2$).

ARBSs exhibited a ligand-dependent increase in expression levels by >2-fold compared with a vehicle-treated control by 48 h after treatment. Among them, UGT1A1 and Pepsinogen C (PGC) levels elevated by >30- and >1000-fold, respectively, with 48-h R1881 treatment (Figure 3a and b). Residual two of 10 genes adjacent to the ARBSs, SCAP2 and MET, exhibited a ligand-dependent decrease in expression levels (Figure 3c).

UGT1A gene locus encodes nine distinct isoforms with unique exon 1 based on the difference of TSSs (Gong *et al.*, 2001). Individual first exons are determinants for the structure of N-terminal UGT1A isoforms, which are important for substrate specificity. We examined whether androgen regulated the transcription of distinct UGT1A isoforms in LNCaP cells. Interestingly, only the mRNA levels of UGT1A1 (Figure 3a) and UGT1A3 isoforms, which have TSSs most adjacent to ARBS no. 1, were significantly increased up to 48 h after R1881 (10 nM) stimulation (UGT1A3 mRNA levels: 1.2±0.1 fold at 12 h, 5.8±0.2 fold at 24 h and 11.2±0.2 fold at 48 h after treatment). On the contrary, the mRNA levels of other UGT1A isoforms were not basically altered or rather decreased during the time course (data not shown).

Taken together, our data suggest that AR could regulate transcription of genes adjacent to ARBSs.

ARBSs are associated with histone acetylation and facilitate recruitment of RNA PolII

We next examined whether these ARBS regions recruited components indicative of transcriptional activation. ChIP analyses for acetylated histone H3/H4 (AcH3/H4) and RNA PolII were performed on the 10 ARBS regions in LNCaP cells (Figure 4). The AREs in PSA promoter and enhancer were used as positive

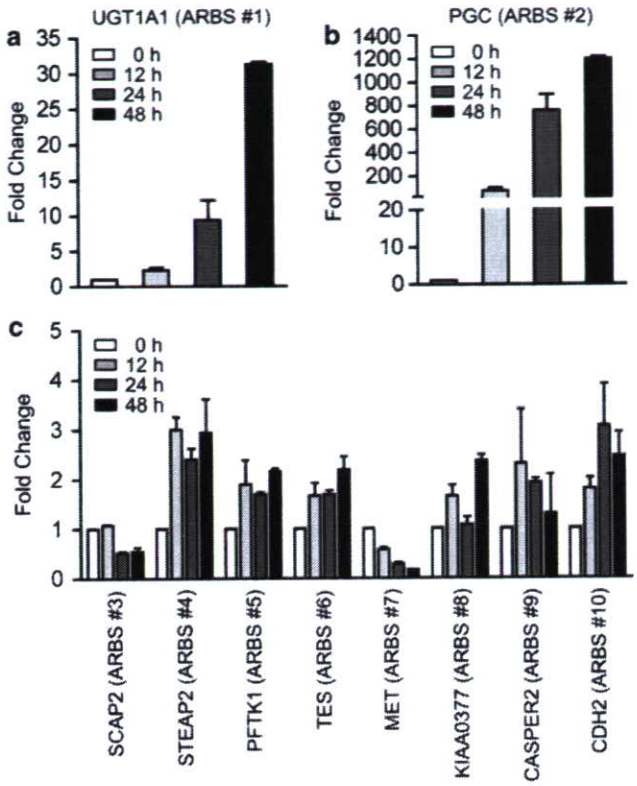

Figure 3 Androgen-dependent changes in expression of genes adjacent to the ChIP-chip ARBSs in LNCaP cells. Hormone-deprivated cells were stimulated with R1881 (10 nM) or vehicle for 12, 24 and 48 h. Quantitative RT–PCR analysis regarding the expression of 10 proximal genes close to ARBSs no. 1–no. 10 was performed using the reverse-transcribed cDNAs from the cells. Data are fold change compared with vehicle-treated cells at individual time point (mean ± s.d., $n = 2$). (**a**) UGT1A1 mRNA levels, (**b**) PGC mRNA levels and (**c**) mRNA levels of gene adjacent to ARBSs no. 3–no. 10.

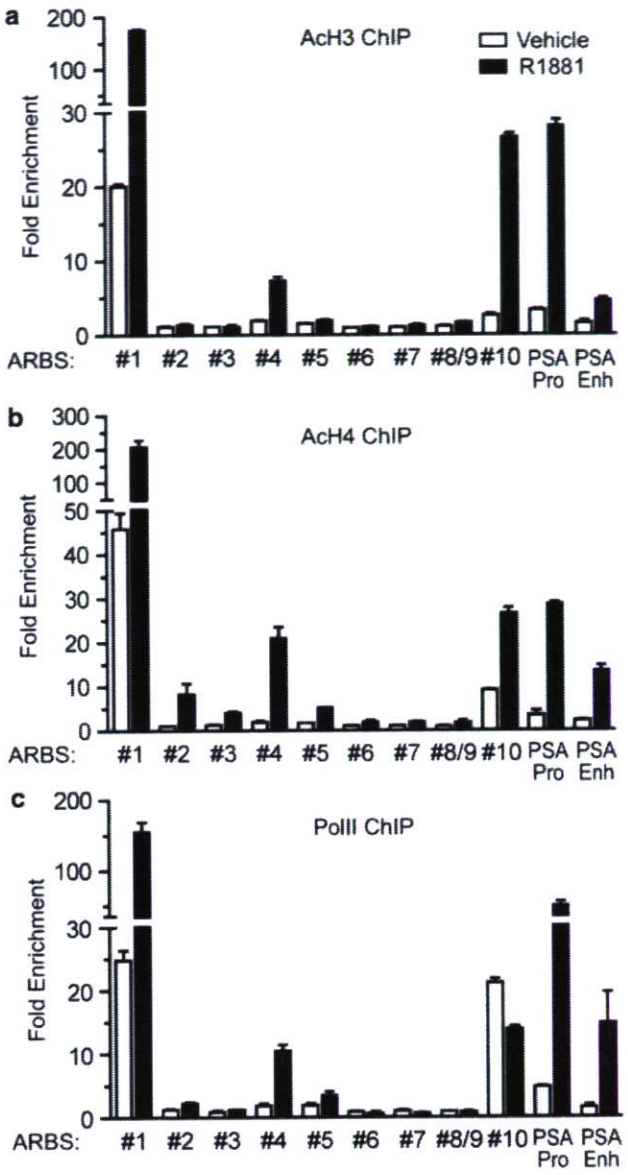

Figure 4 Some of the ChIP-chip ARBSs associate with histone acetylation and RNA PolII recruitment. Hormone-deprivated LNCaP cells were stimulated with R1881 (10 nM) or vehicle for 24 h. Cross-linked samples were immunoprecipitated with anti-acetylated H3/H4 (AcH3/AcH4) or anti-RNA PolII antibodies. The precipitated DNA fragments were subjected to qPCR. Identical primer sets were used as described in Figure 2. Data are fold enrichment compared to individual input non-enriched DNA (mean ± s.d., $n = 2$).

controls. Histone acetylation was remarkable by R1881 treatment in ARBSs no. 1 and no. 10, in the vicinity of UGT1A1 and CDH2, respectively. Ligand-dependent RNA PolII recruitment was also significant in ARBS no. 1. In ARBS no. 10, PolII binding was enriched at basal levels and further enhancement of PolII binding was not observed by ligand stimulation (Figure 4c). Moderate histone acetylation and PolII recruitment in response to R1881 were also observed in ARBS no. 4, which was located in intron 3 of STEAP2. In the rest of seven ARBSs, all associated with ligand-dependent AcH3/H4 binding by >2-fold and three of seven recruited PolII ligand dependently by >2-fold. Although most of the identified ARBSs were located rather distal from known genes, our data suggest that a significant number of the ARBSs in the genome physically function as distal transcriptional regulatory domains during transcription of the adjacent genes.

Functional recruitment of p160 co-activators at ARBSs

The p160 SRC family co-activators play scaffold roles in forming co-activator complex involved in nuclear receptor-mediated transcription (Shang and Brown, 2002). In AR-mediated transcription, the p160 co-activators are shown to be recruited to AR complex and to facilitate AR transactivation by their histone acetylase activity (Shang *et al*., 2002). To delineate the functional roles of endogenous p160 co-activators in AR-mediated transcription from the identified ARBSs no. 1–no. 10, we performed ChIP analysis using antibodies against SRC1, GRIP1 and AIB1 (Figure 5). It is notable that all of the p160 co-activators were recruited by >10-fold in the ARE from PSA promoter.

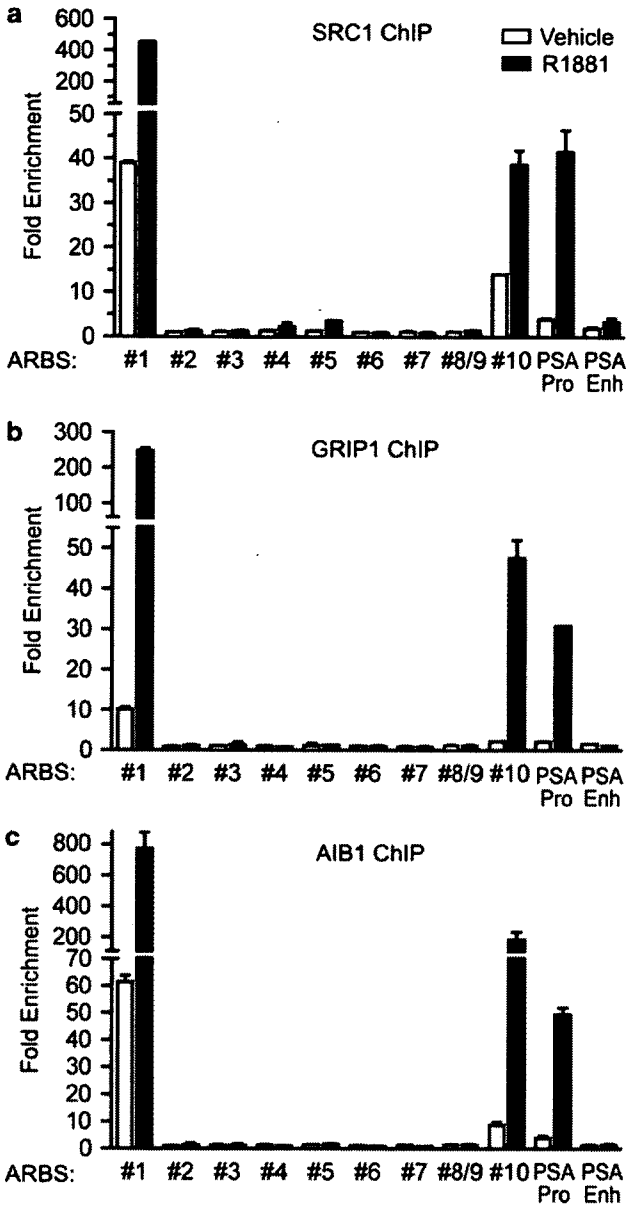

Figure 5 ChIP-chip ARBSs and p160 coactivator recruitment. Hormone-deprivated LNCaP cells were stimulated with R1881 (10 nM) or vehicle for 24 h. Cross-linked samples were immunoprecipitated with anti-SRC1, anti-GRIP1 or anti-AIB1 antibodies. The precipitated DNA fragments were subjected to qPCR. Identical primer sets were used as described in Figure 2. Data are fold enrichment compared to individual input non-enriched DNA (mean ± s.d., $n = 2$).

Consistent with the result of histone acetylation and RNA PolII recruitment, all of the p160 co-activators were recruited by >10-fold upon R1881 stimulation compared with vehicle in ARBS no. 1, adjacent to UGT1A1. The second potent binding site for AcH3/H4 and RNA PolII, ARBS no. 10 adjacent to CDH2, recruited SRC1 by >2-fold and GRIP1 and AIB1 by >20-fold upon ligand stimulation. Among other ARBSs, ARBS no. 5 close to PFTK1 recruited SRC1 by >2-fold in response to ligand stimulation. The data show that some of the authentic ARBSs may play roles as enhancers that recruit various transcriptional regulators and co-activators.

Distal and intronic ARBSs function as transcriptional regulators in androgen-dependent transcription

To further assess the possibility that the distal or intronic ARBSs function as bona fide transcriptional regulators in androgen-dependent transcription, we performed promoter activity assay using luciferase reporter constructs including ARE sequences derived from the ARBSs. Using the genomic DNA of LNCaP cells as a template, we amplified fragments included ARE sequences in ARBSs no. 1 and no. 10, corresponding to the 5′ upstream region of UGT1A1 (~−17 kb) and intron 1 of CDH2 (Figure 6a and b). Note that ARBS no. 1 is also located in intron 1 of other UGT1A isoforms. The amplified fragments were ligated to a luciferase reporter plasmid pGL3-vector containing SV40 promoter. Regarding the 5′ upstream region of UGT1A1, we also generated a mutated construct including two substitutions at the positions −2C and +2G from the 3-bp spacer (UGT1A1 5′ Mut-Luc). Using LNCaP cells transfected with reporter constructs, the luciferase activities of UGT1A1 5′-Luc and CDH2 Int 1-Luc were increased ~5- and ~8-fold by R1881 treatment, respectively, whereas MMTV luciferase construct exhibited >100-fold activation in response to ligand stimulation (Figure 6c). UGT1A1 5′ Mut-Luc did not exhibit androgen-dependent transcriptional activation. These results suggest that a significant number of non-promoter ARBSs also play essential roles in AR-mediated gene transcription.

Moreover, UGT1A protein expression could be regulated by androgen (Figure 6d). LNCaP cells after 72-h hormone deprivation were stimulated with R1881 or vehicle and cell lysates were prepared after 24 or 48 h. Although the isoform specificity of UGT1A was not shown by the antibody that we used, overall amounts of UGT1A protein were increased in response to androgen.

Discussion

This study aimed to identify novel androgen target genes in prostate cancer LNCaP cells by performing ChIP-chip analysis, identifying *in vivo* ARBSs in the selected ENCODE genomic regions. This scanning successfully identified 10 bona fide *in vivo* ARBSs with a $P < 1e\text{-}5$. Notably, all of the 10 ARBSs included ARE sequences as determined by the sequence analysis utilities based on TRANSFAC or JASPER transcription factor-binding profiles (Matys *et al.*, 2003; Sandelin *et al.*, 2004), and ChIP-PCR validation confirmed that those ARBSs had abilities to recruit AR ligand dependently. Our ChIP-chip approach is a powerful high-throughput method that can be applied to the whole genome-wide screen of ARBSs.

Efforts have been paid to identify transcription factor-binding motifs for years by searching a consensus-like sequence through *in silico* or *in vitro* studies in

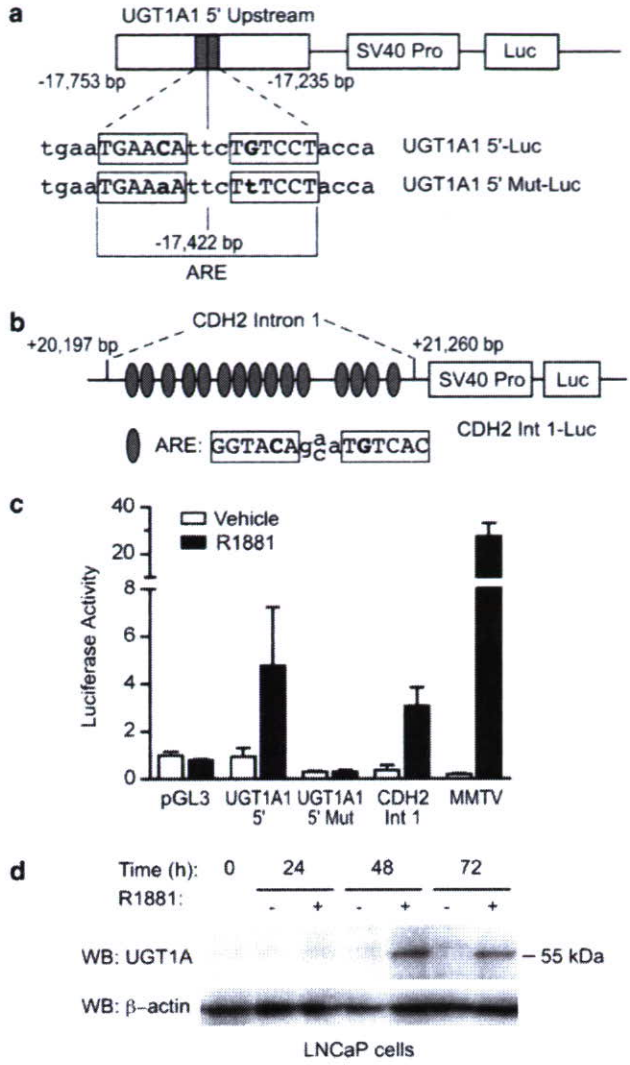

Figure 6 Transcriptional activity of UGT1A1 5′ upstream and CDH2 intronic ARBSs. (**a**) Construction of luciferase reporter plasmids containing UGT1A1 5′ upstream regions. A 519-bp fragment of the 5′ upstream of UGT1A1 (−17 753/−17 235 bp) amplified from LNCaP cells, and the 5′ fragment of UGT1A1 with mutation at the positions −2C and +2G from the 3-bp spacer in ARE sequences (ARBS no. 1) were cloned into pGL3 vector containing SV40 promoter (SV40 Pro), designated as UGT1A1 5′-Luc and UGT1A1 5′ Mut-Luc, respectively. (**b**) Construction of luciferase reporter plasmid containing CDH2 intron 1. A genomic fragment of CDH2 intron 1 (ARBS no. 10) derived from LNCaP cells (+20 197/+21 260 bp), containing 15 repeats of palindromic ARE sequences with the half-site GGTACA, was cloned into pGL3 vector (CDH2 Int 1-Luc). Note that the number of ARE sequences in LNCaP cells was larger than that in the genome database. (**c**) Androgen-stimulated luciferase activities of ARE sequences involved in UGT1A1 5′ upstream and CDH2 intron 1. LNCaP cells were stimulated with R1881 (10 nM) or vehicle 12 h after transfection with indicated plasmids together with a Renilla luciferase reporter gene, and incubated for another 24 h. Firefly luciferase activity was normalized to Renilla luciferase activity for each data set. MMTV luciferase reporter gene containing ARE sequences was used as a positive control. Data represent the mean ± s.d., $n = 3$. (**d**) Androgen-stimulated expression of UGT1A protein in LNCaP cells. Cells were stimulated with R1881 (10 nM) or vehicle for indicated times and whole cell lysates were separated by 8% SDS–PAGE. The PVDF membrane blotted with proteins were probed with anti-UGT1A or anti-β-actin antibodies.

the vicinity of transcription factor targets. In the days after the completion of the Human Genome Project, genomic DNA microarray has been developed and identification of *in vivo* binding targets of nuclear proteins is enabled by ChIP-chip analysis. For instance, in the ChIP-chip study for ERα on chromosomes 21 and 22, most of the binding sites were found at significant distances including several > 100 kb removed from TSSs (Carroll *et al*., 2005). It has been suggested that these distal ERα-binding sites play an important role in estrogen-mediated regulation, as they could be physically associated with promoter-proximal regions. Similarly, in the present study, nine of 10 ARBSs that we identified by ChIP-chip were situated in the distal 5′ regions or intronic regions of known genes. Among those distal ARBSs, there were several sites that significantly recruited AcH3/H4 and RNA PolII (Figure 4). ARBSs no. 1 and no. 10, which are located at > 17 kb upstream of UGT1A1 and in intron 1 of CDH2, respectively, could also associate with the p160 co-activators in a ligand-dependent manner (Figure 5). Based on our findings and previous evidence, a number of ARBSs may be located in non-promoter regions of the genome, and often associated with histone acethylation and co-activator recruitment.

In the vicinity of ChIP-chip identified ARBSs, we found several genes upregulated or downregulated by androgen stimulation. PGC, whose location is close to ARBS no. 2, is an androgen-upregulated gene that has been reported previously as a prognostic factor in prostate cancer (Diaz *et al*., 2002). It is an aspartyl protease and known as a protein involved in the digestion of proteins in the stomach. We identified a novel ARE sequence in ARBS no. 2, at −323 bp upstream of the TSS of PGC, indicating that ChIP-chip is particularly a powerful method to find out a novel transcription factor target regardless of the expression level of the target gene. As the ligand-dependent RNA PolII recruitment was not significant at ARBS no. 2 at the time we investigated (Figure 4c), other PGC regulatory region might be more important in the PolII activation; yet, ARBS no. 2 might play a role in the transcriptional regulation of PGC as the histone acetylation was at least promoted by ligand stimulation (Figure 4b). STEAP2, which includes ARBS no. 4 in intron 3, has been originally cloned as a STEAP homolog gene that encodes a transmembrane protein expressed in prostate cancer (Porkka *et al*., 2002). Although androgen responsiveness of STEAP2 was not reported previously, our data showed that it was a novel androgen target gene with a genuine ARBS in intron 3, which was also associated with histone acetylation.

ENCODE region ENm001 corresponds to chromosome 7q31, which is known as a fragile site with frequent loss of heterozygosity in advanced prostate cancer (Kawana *et al*., 2002). Among several genes at 7q31, TES (testis-derived transcript) has been shown as a candidate tumor suppressor gene in prostate cancer (Chene *et al*., 2004). In the present studies, we showed that TES was an androgen-upregulated gene with a

genuine ARBS (ARBS no. 6) in its 3′ downstream region (−58 kb from the 3′-end). TES protein contains three conserved cysteine-rich zinc-binding motifs called LIM domains, suggesting that TES may play a role in protein-protein interaction and focal adhesion (Coutts *et al.*, 2003). Methylation of the CpG island at the 5′ end of TES is frequently occurred in ovarian cancer cells, and overexpression of TES in culture cells was shown to be growth-inhibitory (Tobias *et al.*, 2001). In contrast, we showed that MET was an androgen-downregulated gene with a novel ARBS (ARBS no. 7) in intron 17. MET encodes a receptor-like tyrosine kinase, c-met proto-oncogene product, which can be activated by hepatocyte growth factor as a receptor (Cooper *et al.*, 1984). It has been reported that MET expression is upregulated by androgen deprivation and MET appears to be preferentially expressed in androgen-insensitive, high-grade prostate cancer cells (Pisters *et al.*, 1995; Humphrey *et al.*, 1995). It has been also shown that overexpression of AR in prostate cancer PC3 cells leads to MET downregulation (Maeda *et al.*, 2006). Based on our bindings, we could propose that both TES and MET at 7q31 are regulated by AR in a way to exhibit negative feedback for prostate cancer progression, while the former is a tumor suppressor gene and the latter is a proto-oncogene.

CDH2 encodes one of the calcium-dependent cell adhesion molecules, N-cadherin. Whereas another calcium-dependent cell adhesion molecules, E-cadherin, is expressed in epithelial cells, N-cadherin is expressed in nerve system, skeletal muscle and mesenchymal cells (Jaggi *et al.*, 2006). Recent evidence suggests that changes in cadherin expression or cadherin switching play a critical role during progression of various tumors including breast cancer (Hazan *et al.*, 1997) and prostate cancer (Tomita *et al.*, 2000). Loss of E-cadherin expression was seen in high-grade breast and prostate cancers, whereas high levels of N-cadherin expression was shown in invasive tumors. Androgen responsiveness of N-cadherin has been shown in neurons, in spinal motoneurons (Monks and Watson, 2001). Our finding demonstrates that CDH2 is an androgen target gene with a novel cluster of ARE repeats in intron 1.

Interestingly, we found a polymorphism in terms of the number of ARE sequences in intron 1 of CDH2. In regard to the 15-bp complete palindromes consisting of the half-site GGTACA motif, LNCaP cells had 15 ARE sequences as shown in Figure 6b, whereas the genomic data published in NCBI Genome Browser contained 13 ARE sequences. We also found that 15 and 14 ARE repeats were contained in the CDH2 intron 1 derived from prostate cancer DU145 cells and benign prostate hyperplasia BPH1 cells, respectively (data not shown). By generating luciferase constructs including the ARE repeats of the CDH2 intron 1 derived from DU145 and BPH1, we showed that the luciferase activities of those constructs were also induced by R1881 stimulation, although the response of BPH1 was smaller than that of LNCaP or DU145. Thus, the polymorphism of ARE repeats in intron 1 may be related to the intensity of androgen responsiveness.

In this study, we demonstrated that UGT1A was a novel androgen-regulated gene with a functional ARE sequence in the 5′ upstream region of UGT1A1 or intron 1 in other UGT1A isoforms. Among several UGT1A isoforms, only UGT1A1 and UGT1A3 have been shown as androgen-upregulated genes in LNCaP cells. Considering out results, it is possible that the isoform-specific androgen responsiveness is linked with the closeness of the functional ARE in ARBS no. 1 to each isoform TSS. Thus, ChIP-chip would be also useful to dissect the isoform specificity of transcription factor target genes that encode a number of isoforms.

The human UGT1A locus spans ~200 kb on chromosome 2q37 and encodes nine UGT1A enzymes that play a crucial role in glucuronidation of xenobiotics and endobiotic substrates such as bilirubin (Chen *et al.*, 2005). UGT1A proteins are expressed in liver, whereas also expressed in extrahaptic tissues like urinary bladder and large intestine (Giuliani *et al.*, 2005). UGT1A gene products are generated by a strategy of exon sharing, resulting in divergent isoforms with a unique N-terminal domain and commonly shared C-terminal 245 amino acids. As UGT proteins are detoxifying enzymes, it is natural that this gene expression is regulated by xenobiotic receptor including pregnenolone X receptor and constitutive androstane receptor (Sugatani *et al.*, 2001; Xie *et al.*, 2003). Reduction of UGT1A expression is involved in the early phase of neoplastic transformation, such as in liver and biliary cancer, bladder cancer and colon cancer (Strassburg *et al.*, 1997; Giuliani *et al.*, 2005). In contrast, decrease in UGT1A1 expression seems to be associated with the reduced risk of endometrial cancer (Duguay *et al.*, 2004). UGT1A1 promoter polymorphism with an $A(TA)_7TAA$ element instead of a normal $A(TA)_6TAA$ element is known to decrease the level of gene expression, and it has been shown that there was a significant inverse association with the seven dinucleotide repeat allele and endometrial cancer risk (Duguay *et al.*, 2004). UGT proteins also glucuronidate steroid hormones, as the UGT1A enzymes showing specificity for estrogens, whereas androgens are substrates for another type of UGT family, UGT2B proteins (Lepine *et al.*, 2004). It has been recently shown that UGT2B15 isoform is an estrogen-regulated gene that is involved in the glucuronidation of androgens as well as estrogens (Harrington *et al.*, 2006). Similarly, there is a possibility that UGT1A1 and UGT1A3 play a role in glucuronidation of androgens as well as estrogens.

In summary, we performed ChIP-chip analysis for *in vivo* ARBSs in prostate cancer LNCaP cells, on the ENCODE regions in the human genome. A number of novel androgen target genes were identified adjacent to the ChIP-chip-based ARBSs. The present results show that ChIP-chip has an advantage over transcript-based microarray analysis, identifying a number of bona fide AR target genes regardless of their expression levels based on the data of functional ARBSs. The androgen target genes identified by the present study would play various important roles in the maintenance of prostate cancer, including detoxification, protein degradation,

cell motility/migration and tumor suppression/progression. Our study could be extended to the whole genome search of ARBSs in different cell systems using various ligands for the receptor. Identification of novel androgen target genes by ChIP-chip will reveal the whole entity of androgen signaling network, and will be applied to develop new clinical methods of prevention, diagnosis and treatment for prostate cancer.

Materials and methods

Reagents

Methyltrienolone 17β-hydroxy-17α-methyl-estra-4,9,11-trien-3-one (R1881) was purchased from NEN Life Science Products (Boston, MA, USA). Anti-AR (H-280), anti-SRC1 (M341), anti-GRIP1 (M343), anti-UGT1A (H-300) antibodies were purchased from Santa Cruz Biotechnology (Santa Cruz, CA, USA). Anti-AcH3 and anti-AcH4 were from Upstate Biotechnology (Lake Placid, NY, USA). Anti-RNA PolII (8WG16) was from Covance (Berkeley, CA, USA). Anti-β-actin monoclonal antibody was from Sigma (St Louis, MO, USA). Anti-AIB1 antibody was generated from rabbit serum using a glutathione *S*-transferase fusion protein with amino acids 1320–1420 of human AIB1 protein as an epitope.

Cell culture

Human prostate cancer LNCaP cells were purchased from American Type Culture Collection (Rockville, MD, USA). Cells were maintained in RPMI 1640 supplemented with 4.5 g/dl glucose, 1 mM sodium pyruvate, 10 mM HEPES and 10% fetal bovine serum (FBS). Before hormone addition, cells were cultured for 2 days in phenol red-free RPMI 1640 with 5% dextran-charcoal stripped FBS (dcc-FBS) and 1 day in phenol red-free medium supplemented with 2.5% dcc-FBS.

Chromatin immunoprecipitation

ChIP assay and qPCR were performed as previously described (Horie-Inoue *et al*., 2004, 2006). LNCaP cells after 72-h hormone depletion were treated with 10 nM R1881 or vehicle (0.1% ethanol) for the indicated times. Cells were fixed in 1% formaldehyde for 5 min at room temperature. Chromatin was sheared to an average size of 500 bp by sonication using a Bioruptor ultrasonicator (Cosmo-Bio, Tokyo, Japan). Lysates were rotated at 4°C for overnight with specific antibodies. Salmon sperm DNA/protein A–agarose (Upstate Biotechnology, Lake Placid, NY, USA) was added and incubated for 2 h. Precipitated DNA was used as templates for qPCR using Applied Biosystems 7000 sequence detector (Foster City, CA, USA) based on SYBR Green I fluorescence. Genomic fragments containing ARE in the promoter and enhancer regions of PSA (−250/−39 bp and −4170/−3978 bp from the TSS, respectively) were used as positive controls for AR binding (Horie-Inoue *et al*., 2004). Sequences of PCR primers are described in Supplementary Table 1.

DNA amplification and microarray preparation

ChIP-enriched DNA was amplified by two-step IVT as described previously (Katou *et al*., 2006). Briefly, alkali phosphatase-treated ChIP DNA was incubated with terminal transferase for poly-dT tailing, annealed with T7-poly A primer (5′-GCATTAGCGGCCGCGAAATTAATACGACTCACTATAGGGAGAAAAAAAAAAAAAAAAA[C/T/G]-3′), and used as a template for second-strand cDNA synthesis. Using this template DNA, first IVT amplification was performed by T7 RNA polymerase (Ambion Inc., Austin, TX, USA). The first-strand cDNA was synthesized using the amplified cRNA as a template. Second-strand cDNA synthesis and IVT amplification were carried out again. Second amplified RNA was converted into double-strand cDNA with random primers, fragmented with DNase I and end labeled with biotin. Hybridization was performed on the Affymetrix GeneChIP ENCODE01 1.0 Arrays (Santa Clara, CA, USA) using 2 μg of ChIP-enriched and non-enriched input control DNA.

Analysis of microarray data

Array intensity data were analysed by the Affymetrix Tiling Analysis Software based on the algorithm by Cawley *et al*. (2004), and the results were mapped to genomic positions in human genome assembly hg 17 (NCBI Build 35) or in Affymetrix Integrated Genome Browser. In ENCODE01 1.0 Arrays, sets of one probe pair, a perfect matched (PM) probe and a mismatch probe (MM) both 25 bases long are tiled at an average resolution of 22 bp as measured from the central position of adjacent 25-mer oligos, creating an overlap of approximately 3 bp. The (PM-MM) intensity value was recorded for each probe pair as a new probe value, and the distribution of probe value was adjusted to equal across all samples by conducting quantile normalization on each duplicate arrays for two groups, including non-enriched genomic input DNA or ChIP-enriched DNAs by AR antibody. To determine whether a probe x is ChIP-enriched, Wilcoxon rank sum test was applied to rank all the probe pairs within a 550-bp sliding window from x by their $\log_2$(max(PM-MM),1) values for checking whether the sum of ranks of all probe pairs in the ChIP samples were significantly higher than that in the controls (a P-value cutoff of 1e-5). For each window, a signal ratio was also estimated by the Hedges–Lehmann method computing the median of folds enrichment among the probe sets within the window.

Reverse transcription-qPCR

Total RNA was extracted from hormone-treated or 0.1% ethanol-treated cells for indicated times using ISOGEN reagent (Nippon Gene, Tokyo, Japan). First strand cDNA was generated from RNase-free DNase I-treated total RNA by using SuperScript II Reverse Transcriptase (Invitrogen, Carlsbad, CA, USA) and oligo-dT_{20} primer. Androgen responsiveness was analysed by quantitative reverse transcription-PCR (RT-qPCR) using Applied Biosystems 7000 sequence detector based on SYBR Green I fluorescence. Primer design and PCR protocol were as previously described (Horie-Inoue *et al*., 2004, 2006). Sequences of PCR primers are described in Supplementary Table 2.

Sequence analysis

The sequences of human RefSeq transcripts (hg 17, NCBI build 35) were retrieved from UCSC genome browser (http://www.genome.ucsc.edu/) (Kent *et al*., 2002). The presence of ARE sequences in the genomic DNA of every ChIP-enriched region were determined by a position weighted matrix method TRANSFAC (Matys *et al*., 2003) with the matrix conservation >75%. If no ARE sequence was predicted by this criteria, the search was performed by a sequence analysis utility of JASPER, an open-access database for eukaryotic transcription factor binding profiles, with the relative profile score threshold >70% (Sandelin *et al*., 2004).

Luciferase assay

Luciferase reporter genes containing ARE sequences in ARBSs no. 1 and no. 10 identified by ChIP-chip were constructed by ligating the fragments derived from UDP-glucuronosyltransferase (UGT) 1A1 5′ upstream region (−17 753/−17 235 bp from the TSS) and cadherin-2 (CDH2) intron 1 region (+20 197/+21 260 bp from the TSS) into pGL3 vector (Promega, Madison, WI, USA) at the sites between *Mlu*I and *Xho*I, designated as UGT1A1 5′-Luc and CDH2 Int 1-Luc, respectively. A mutated UGT1A1 5′ region construct (UGT1A1 5′ Mut-Luc) was also generated, including the identical region of UGT1A1 5′-Luc except two substitutions of conserved C and G for A and T, respectively, at the 2-bp apart positions from the 3-bp spacer of ARE sequence. Mouse mammary tumor virus luciferase construct (MMTV-Luc) was used as a positive control for AR transcription activity (Ogawa *et al.*, 1995). LNCaP cells were plated at a density of 10 000 cells/well in a 24-well culture plate and cultured for 3 days in phenol red-free RPMI 1640 with 5% dcc-FBS. Cells were transfected with plasmids using the transfection reagent FuGENE6 (Roche Applied Science, Indianapolis, IN, USA), then 12 h later treated with R1881 (10 nM) or vehicle (0.1% ethanol) for 24 h. Luciferase activity of cell lysate was determined by the Dual Luciferase Assay Kit (Promega, Madison, WI, USA). A renilla luciferase reporter Tk-PRL was co-transfected as a control for evaluating transfection efficiency. Data represent means ± s.d. from triplicate sets.

Western blotting

Whole cell lysates were prepared using lysis buffer (50 mM Tris–HCl, pH 8.0, 150 mM NaCl, 1% TritonX-100, 1.5 mM $MgCl_2$, 10 μg/ml aprotinin, 10 μg/ml leupeptin, 1 mM PMSF). Protein concentrations were analyzed using the BCA protein assay kit (Pierce Biotechnology, Rockford, IL, USA). Fifty microgram of proteins were resolved by 8% SDS–polyacrylamide gel electrophoresis and electroblotted onto Immobilon-P Transfer Membrane (Millipore, Billerica, MA, USA). Membranes were incubated with primary antibodies followed by incubation with secondary antibodies. Antibody–antigen complexes were detected using the Western Blotting Chemiluminescence Luminol Reagent (Santa Cruz Biotechnology, Santa Cruz, CA, USA).

Acknowledgements

We thank T Suzuki and R Nozawa for their technical assistance. This work was supported in part by grants-in-aid from the Ministry of Health, Labor and Welfare; from the Japan Society for the Promotion of Science; from The Promotion and Mutual Aid Corporation for Private Schools of Japan. This work was supported in part by a grant of the Genome Network Project from the Ministry of Education, Culture, Sports, Science and Technology.

References

Bernstein BE, Kamal M, Lindblad-Toh K, Bekiranov S, Bailey DK, Huebert DJ *et al.* (2005). Genomic maps and comparative analysis of histone modifications in human and mouse. *Cell* **120**: 169–181.

Carroll JS, Liu XS, Brodsky AS, Li W, Meyer CA, Szary AJ *et al.* (2005). Chromosome-wide mapping of estrogen receptor binding reveals long-range regulation requiring the forkhead protein FoxA1. *Cell* **122**: 33–43.

Cawley S, Bekiranov S, Ng HH, Kapranov P, Sekinger EA, Kampa D *et al.* (2004). Unbiased mapping of transcription factor binding sites along human chromosomes 21 and 22 points to widespread regulation of noncoding RNAs. *Cell* **116**: 499–509.

Chen CD, Welsbie DS, Tran C, Baek SH, Chen R, Vessella R *et al.* (2004). Molecular determinants of resistance to antiandrogen therapy. *Nat Med* **10**: 33–39.

Chen S, Beaton D, Nguyen N, Senekeo-Effenberger K, Brace-Sinnokrak E, Argikar U *et al.* (2005). Tissue-specific, inducible, and hormonal control of the human UDP-glucuronosyltransferase-1 (UGT1) locus. *J Biol Chem* **280**: 37547–37557.

Chene L, Giroud C, Desgrandchamps F, Boccon-Gibod L, Cussenot O, Berthon P *et al.* (2004). Extensive analysis of the 7q31 region in human prostate tumors supports TES as the best candidate tumor suppressor gene. *Int J Cancer* **111**: 798–804.

Cooper CS, Park M, Blair DG, Tainsky MA, Huebner K, Croce CM *et al.* (1984). Molecular cloning of a new transforming gene from a chemically transformed human cell line. *Nature* **311**: 29–33.

Coutts AS, MacKenzie E, Griffith E, Black DM. (2003). TES is a novel focal adhesion protein with a role in cell spreading. *J Cell Sci* **116**: 897–906.

Diaz M, Rodriguez JC, Sanchez J, Sanchez MT, Martin A, Merino AM *et al.* (2002). Clinical significance of pepsinogen C tumor expression in patients with stage D2 prostate carcinoma. *Int J Biol Markers* **17**: 125–129.

Duguay Y, McGrath M, Lepine J, Gagne JF, Hankinson SE, Colditz GA *et al.* (2004). The functional UGT1A1 promoter polymorphism decreases endometrial cancer risk. *Cancer Res* **64**: 1202–1207.

ENCODE Project Consortium, EP (2004). The ENCODE (ENCyclopedia of DNA Elements) Project. *Science* **306**: 636–640.

Giuliani L, Ciotti M, Stoppacciaro A, Pasquini A, Silvestri I, De Matteis A *et al.* (2005). UDP-glucuronosyltransferases 1A expression in human urinary bladder and colon cancer by immunohistochemistry. *Oncol Rep* **13**: 185–191.

Gong QH, Cho JW, Huang T, Potter C, Gholami N, Basu NK *et al.* (2001). Thirteen UDP glucuronosyltransferase genes are encoded at the human UGT1 gene complex locus. *Pharmacogenetics* **11**: 357–368.

Grossmann ME, Huang H, Tindall DJ. (2001). Androgen receptor signaling in androgen-refractory prostate cancer. *J Natl Cancer Inst* **93**: 1687–1697.

Harrington WR, Sengupta S, Katzenellenbogen BS. (2006). Estrogen regulation of the glucuronidation enzyme UGT2B15 in estrogen receptor-positive breast cancer cells. *Endocrinology* **147**: 3843–3850.

Hazan RB, Kang L, Whooley BP, Borgen PI. (1997). N-cadherin promotes adhesion between invasive breast cancer cells and the stroma. *Cell Adhes Commun* **4**: 399–411.

Horie-Inoue K, Bono H, Okazaki Y, Inoue S. (2004). Identification and functional analysis of consensus androgen response elements in human prostate cancer cells. *Biochem Biophys Res Commun* **325**: 1312–1317.

Horie-Inoue K, Takayama K, Bono HU, Ouchi Y, Okazaki Y, Inoue S. (2006). Identification of novel steroid target genes through the combination of bioinformatics and functional analysis of hormone response elements. *Biochem Biophys Res Commun* **339**: 99–106.

Humphrey PA, Zhu X, Zarnegar R, Swanson PE, Ratliff TL, Vollmer RT *et al.* (1995). Hepatocyte growth factor and its

receptor (c-MET) in prostatic carcinoma. *Am J Pathol* **147**: 386–396.

Jaggi M, Nazemi T, Abrahams NA, Baker JJ, Galich A, Smith LM *et al.* (2006). N-cadherin switching occurs in high Gleason grade prostate cancer. *Prostate* **66**: 193–199.

Katou Y, Kaneshiro K, Aburatani H, Shirahige K. (2006). Genomic approach for the understanding of dynamic aspect of chromosome behavior. *Methods Enzymol* **409**: 389–410.

Kawana Y, Ichikawa T, Suzuki H, Ueda T, Komiya A, Ichikawa Y *et al.* (2002). Loss of heterozygosity at 7q31.1 and 12p13-12 in advanced prostate cancer. *Prostate* **53**: 60–64.

Kent WJ, Sugnet CW, Furey TS, Roskin KM, Pringle TH, Zahler AM *et al.* (2002). The human genome browser at UCSC. *Genome Res* **12**: 996–1006.

Laganière J, Deblois G, Lefebvre C, Bataille AR, Robert F, Giguère V. (2005). From the cover: location analysis of estrogen receptor alpha target promoters reveals that FOXA1 defines a domain of the estrogen response. *Proc Natl Acad Sci USA* **102**: 11651–11656.

Lepine J, Bernard O, Plante M, Tetu B, Pelletier G, Labrie F *et al.* (2004). Specificity and regioselectivity of the conjugation of estradiol, estrone, and their catecholestrogen and methoxyestrogen metabolites by human uridine diphosphoglucuronosyltransferases expressed in endometrium. *J Clin Endocrinol Metab* **89**: 5222–5232.

Maeda A, Nakashiro K, Hara S, Sasaki T, Miwa Y, Tanji N *et al.* (2006). Inactivation of AR activates HGF/c-Met system in human prostatic carcinoma cells. *Biochem Biophys Res Commun* **347**: 1158–1165.

Matys V, Fricke E, Geffers R, Gossling E, Haubrock M, Hehl R *et al.* (2003). TRANSFAC: transcriptional regulation, from patterns to profiles. *Nucleic Acids Res* **31**: 374–378.

Monks DA, Watson NV. (2001). N-cadherin expression in motoneurons is directly regulated by androgens: a genetic mosaic analysis in rats. *Brain Res* **895**: 73–79.

Ogawa H, Inouye S, Tsuji FI, Yasuda K, Umesono K. (1995). Localization, trafficking, and temperature-dependence of the Aequorea green fluorescent protein in cultured vertebrate cells. *Proc Natl Acad Sci USA* **92**: 11899–11903.

Pisters LL, Troncoso P, Zhau HE, Li W, von Eschenbach AC, Chung LW. (1995). c-met Proto-oncogene expression in benign and malignant human prostate tissues. *J Urol* **154**: 293–298.

Porkka KP, Helenius MA, Visakorpi T. (2002). Cloning and characterization of a novel six-transmembrane protein STEAP2, expressed in normal and malignant prostate. *Lab Invest* **82**: 1573–1582.

Sandelin A, Alkema W, Engstrom P, Wasserman WW, Lenhard B. (2004). JASPAR: an open-access database for eukaryotic transcription factor binding profiles. *Nucleic Acids Res* **32**: D91–94.

Shang Y, Brown M. (2002). Molecular determinants for the tissue specificity of SERMs. *Science* **295**: 2465–2468.

Shang Y, Myers M, Brown M. (2002). Formation of the androgen receptor transcription complex. *Mol Cell* **9**: 601–610.

Strassburg CP, Manns MP, Tukey RH. (1997). Differential down-regulation of the UDP-glucuronosyltransferase 1A locus is an early event in human liver and biliary cancer. *Cancer Res* **57**: 2979–2985.

Sugatani J, Kojima H, Ueda A, Kakizaki S, Yoshinari K, Gong QH *et al.* (2001). The phenobarbital response enhancer module in the human bilirubin UDP-glucuronosyltransferase UGT1A1 gene and regulation by the nuclear receptor CAR. *Hepatology* **33**: 1232–1238.

Tobias ES, Hurlstone AF, MacKenzie E, McFarlane R, Black DM. (2001). The TES gene at 7q31.1 is methylated in tumours and encodes a novel growth-suppressing LIM domain protein. *Oncogene* **20**: 2844–2853.

Tomita K, van Bokhoven A, van Leenders GJ, Ruijter ET, Jansen CF, Bussemakers MJ *et al.* (2000). Cadherin switching in human prostate cancer progression. *Cancer Res* **60**: 3650–3654.

Wang Q, Carroll JS, Brown M. (2005). Spatial and temporal recruitment of androgen receptor and its coactivators involves chromosomal looping and polymerase tracking. *Mol Cell* **19**: 631–642.

Xie W, Yeuh MF, Radominska-Pandya A, Saini SP, Negishi Y, Bottroff BS *et al.* (2003). Control of steroid, heme, and carcinogen metabolism by nuclear pregnane X receptor and constitutive androstane receptor. *Proc Natl Acad Sci USA* **100**: 4150–4155.

Supplementary Information accompanies the paper on the Oncogene website (http://www.nature.com/onc).

Int. J. Cancer: **120,** 2325–2330 (2007)

Increased expression of estrogen-related receptor α (ERRα) is a negative prognostic predictor in human prostate cancer

Tetsuya Fujimura[1], Satoru Takahashi[1,2]*, Tomohiko Urano[3], Jinpei Kumagai[1], Tetsuo Ogushi[1], Kuniko Horie-Inoue[4], Yasuyoshi Ouchi[3], Tadaichi Kitamura[1], Masami Muramatsu[4] and Satoshi Inoue[3,4]

[1]*Department of Urology, Faculty of Medicine, The University of Tokyo, Bunkyo-ku, Tokyo, Japan*
[2]*Department of Urology, Nihon University Hospital, Itabashi-ku, Tokyo, Japan*
[3]*Department of Geriatric Medicine, Faculty of Medicine, The University of Tokyo, Bunkyo-ku, Tokyo, Japan*
[4]*Research Center for Genomic Medicine, Saitama Medical School, Moroyama-machi, Iruma-gun, Saitama, Japan*

The nuclear receptor ERRα (estrogen-related receptor α) is known to modulate the estrogen-signaling pathway, but the biological significance of ERRα in the prostate remains unclear. We investigated the expression of ERRα in human prostate tissues and cancer cell lines to evaluate the potential roles of the receptor in prostate cancer (PC). Western blot analysis of ERRα was performed in three cell lines of human PC (LNCaP, DU145 and PC-3). The expressions of ERRα in cancerous lesions (n = 106) and benign foci (n = 99) of 106 surgically obtained prostate specimens were evaluated by immunohistochemistry. The relationships between the ERRα expression and clinicopathological features were evaluated. Western blot analysis using the polyclonal anti-ERRα antibody detected a 52 kD band in all three PC cell lines. Positive immunostaining of ERRα in the nuclei was found in 73 (69%) cancerous and 47 (47.5%) benign epithelium, whereas the stromal tissues were negative for ERRα. The mean immunoreactivity score (IR score) of the cancerous lesions (3.5 ± 2.6) was significantly higher than that of the benign foci (1.8 ± 2.1) (p < 0.0001). The IR score of the cancerous lesions significantly correlated with the Gleason score (p = 0.0135). Univariate and multivariate hazard analyses revealed significant correlations between elevated ERRα expression and poor cancer-specific survival (p = 0.0141 and 0.0367, respectively). The enhanced expression of ERRα might play a role in the development of human PC and serve as a significant prognostic factor for the disease.

Key words: estrogen related receptor α (ERRα); prognostic predictor; prostate cancer

Estrogens have been widely used for the treatment of advanced prostate cancer (PC).[1] The direct effect of estrogens on normal prostate and PC is assumed to be mediated through estrogen receptors (ERs) α and β[2,3] ERα is predominantly localized in the stromal cells of the prostate.[3–6] In light of this, the ERα-mediated effects of estrogens on the prostate epithelium are thought to be conferred via paracrine pathways. ERβ, on the other hand, is localized predominantly in the epithelial cell compartment of the normal human prostate, and the expression of ERβ is decreased in PC compared with benign epithelium.[2,3] Thus, ERβ may exert a protective effect against aberrant cell proliferation and carcinogenesis.[7–10]

Recent studies have focused on an additional estrogen signaling pathway mediated by estrogen-related receptors (ERRs) in the estrogen-targeted organs.[11–13] ERRs belong to the nuclear receptor super family and consist of three closely related members (α, β and γ).[11–13] The cDNA for ERRα was isolated by screening cDNA libraries using probes corresponding to the DNA-binding domain of human ERα.[11] Evidence suggests that there may be an overlap between ERRα and ER biology. While ERRα shows no direct response to 17β-estradiol, it has been found to bind to functional estrogen response elements (EREs) in ER target genes such as lactoferrin and aromatase.[12–14] ERRα may participate in processes such as bone development, skeleton formation and fat metabolism.[15–18] Further, ERRα is now established to be associated with unfavorable biomarkers in human breast cancer.[19–21] Much less is known, however, about the extent or pattern of ERRα expression in the prostate.[22] The present study evaluated ERRα expression in human prostate tissues and PC cell lines by immunohistochemistry and Western blot analysis to assess its clinical significance.

Material and methods

Tissue selections and patient characteristics

Formalin-fixed, paraffin-embedded sections were obtained from 106 patients who underwent radical prostatectomy for prostatic adenocarcinoma between 1987 and 2001. We obtained informed consent from all the patients. The age of the patients ranged from 52 to 78 years (mean 66.8 ± 6.0), and pretreatment serum PSA level ranged from 2.2 to 136 ng/ml (mean 16.9 ± 19.5). The pathological stages included B (n = 33), C (n = 59) and D_1 (n = 14). Prostate tissue sections submitted for this study contained 99 benign and 106 cancerous foci. The cancerous lesions consisted of tumors with Gleason score (GS) 6 (n = 22), 7 (n = 41), 8 (n = 20), 9 (n = 22) and 10 (n = 1), which was evaluated by 2 trained pathologists. Thirty-five patients (33%) were treated with surgery alone, whereas the remaining patients received adjuvant antiandrogen therapy. Patients were followed postoperatively by their surgeons at 3-month intervals to 5 years and yearly thereafter. Mean patient follow-up period was 82 ± 39 months (range 10–192). During the follow-up period, 77 patients (73%) are alive with no evidence of the disease, and 12 (11%) are alive with biochemical or clinical recurrence. Eleven patients (10%) died of PC, and 6 (6%) died of other diseases during the follow-up period.

Cell culture

The human prostatic cancer cell lines (PC-3, DU145 and LNCaP) and COS7 cells were obtained from American Type Culture Collection (Rockville, MD) and maintained in the RPMI 1640 with 10% FBS. All cell lines were maintained at 37°C in 5% CO_2. Transfections of hERRα were performed using 3.5 × 10^6 COS7 cells, 5 μg of pcDNA3-hERRα vector and FuGENE® 6 transfection kit (Roche Applied Science, Indianapolis, IN) according to the manufacture's protocol. After 48 hr cell extracts were analyzed.

Antibodies

Rabbit polyclonal antibody for ERR1 (PA1-314) was purchased from Affinity Bio Reagents (Golden, CO). The characterization of this antibody was confirmed by Western blot analysis in hERRα-transfected COS7 cells.

***Correspondence to:** Department of Urology, Nihon University Hospital, 30-1 Oyaguchi, Itabashi-ku, Tokyo 173-8610, Japan.
Fax: +81-3-3972-8111. E-mail: tsatoru@med.nihon-u.ac.jp
Received 30 January 2006; Accepted after revision 9 August 2006
DOI 10.1002/ijc.22363
Published online 9 February 2007 in Wiley InterScience (www.interscience.wiley.com).

Western blot analyses

Western blot analysis was performed using total cell extracts obtained from 3 strains of LNCaP, DU145, PC-3 and hERRα-transfected COS7 cells as previously described.[23] Cells were rinsed twice with ice-cold phosphate-buffered saline (PBS) and lysed in Nonidet P-40 lysis buffer (50 mM Tris-HCl [pH 7.4], 150 mM NaCl, 10 mM NaF, 5 mM EDTA, 5 mM EGTA, 2 mM sodium vanadate, 0.5% sodium deoxycholate, 1 mM diethiothreitol [DTT], 1 mM phenylmethylsulfonyl fluoride [PMSF], 2 mg/ml aprotinin and 0.1% no diet P-40), and the lysates were cleared by centrifugation at 15,000 for 15 min at 4°C. Total protein lysate (20 μg) of each cell line was fractionated on sodium dodecyl sulfate (SDS)-12.5% polyacryl-amide gels and electrophoretically transferred onto polyvinylidene difluoride (PVDF) membranes (Immobilin, Millipore, Bedford, MA). The membranes were blocked in Tris-buffered saline (TBS) with 5% skim milk before incubating with the anti-ERRα antibodies diluted (1:500), followed by a horseradish peroxidase-conjugated donkey anti-rabbit immunoglobulin IgG (Amersham-Pharmacia Biotech, Arlington Heights, IL). Bands were visualized with the chemiluminescence's -based ECL plus detection system (Amersham-Pharmacia Biotech).

Immunohistochemistry

We performed immunohistochemical analysis of ERRα employing the streptavidin-biotin amplification method using a peroxidase catalyzed signal amplification system: CSA system (DAKO, Carpentaria, CA) following the manufacturer-supplied protocol. Tissue-sections (6 μm) were deparaffinized, dehydrated through a graded ethanol series and rinsed in phosphate-buffered saline (PBS). For antigen retrieval, the sections were autoclaved at 120°C for 15 min in citric acid buffer (2 mM citric acid and 9 mM trisodium citrate dehydrate, pH 6.0). After blocking endogenous peroxidase with 0.3% H_2O_2, the sections were incubated in 10% bovine serum for 10 min. Application of the polyclonal antibody for ERRα (1:100 dilution) followed by sequential 15-min incubations with biotinylated link antibody, streptavidin-biotin-peroxidase complex, amplification reagent and streptavidin-peroxidase. The antigen-antibody complex was visualized with 3,3′-diaminobenzidine (DAB) solution (1 mM DAB, 50 mM Tris-HCl buffer pH 7.6 and 0.006% H_2O_2).

As positive controls, sections of human heart tissues (BioChain Institute, Inc, Hayward, CA) were immunoassayed with the primary antibodies in the same manner as described above.

In addition to the standard negative controls with rabbit IgG, we performed peptide blocking of anti-ERRα antibody using its neutralizing peptide purchased from Affinity Bio Reagents (Golden, CO) in order to confirm the specificity of the antibody.

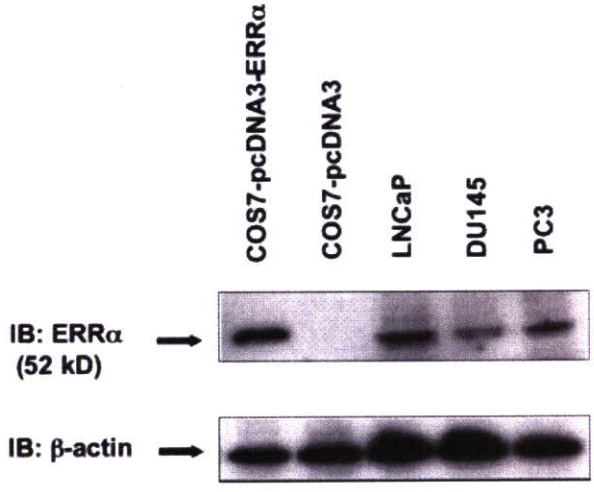

FIGURE 1 – Western blot analysis of the ERRα proteins in pcDNA3-ERRα and PC cell lines (LNCaP, DU145 and PC-3). Total cell extracts were subjected to immunoblotting with both the anti-ERRα and β-actin antibody. Anti-ERRα antibody detected a 52 kD band in COS7-pcDNA3-ERRα and human PC cell lines (LNCaP, DU145 and PC-3).

Immunohistochemical assessment

Immunostained slides were evaluated for the proportion (0, none; 1, <1/100; 2, 1/100 to 1/10; 3, 1/10 to 1/3; 4, 1/3 to 2/3; and 5, >2/3) and the intensity (0, none; 1, weak; 2, moderate; and 3, strong) of positively stained cells.[24] The total scores of immunoreactivity (0–8) were obtained as the sum of the proportion and the intensity. For immunohistochemical assessment, two investigators (T. F. and J. K.) evaluated the tissue sections independently. If IR score was different between two investigators, third investigator (S.T.) counted and we adopted the average IR score. To determine potential correlation between expression of ERRα in the malignant epithelium and clinicopathological characteristics, we considered the sections with 2 of IR score as positive for ERRα immunoreactivity. Since almost all benign foci showed <5 of IR scores for ERRα, we defined IR score 5 as a cutoff for strong immunoreactivity of ERRα.

Statistical analysis

Correlations between the immunoreactivity score (IR score) and clinicopathological characteristics (age, pretreatment serum PSA level, pathological stage and the Gleason score) were evaluated using the *t*-test or chi-square test. Cancer-specific survival curves were obtained by the Kaplan-Meier method and verified by the Log rank (Mantel-Cox) test. We analyzed statistical assessment by Stat View-J 5.0 software (SAS Institute, Cary, NC), and regarded p-values < 0.05 as statistically significant.

Results

Western blot analysis

Using the polyclonal anti-ERRα antibody, a 52 kD band, which corresponded to the molecular weight of ERRα, was detected in COS7-pcDNA3-ERRα. Positive signals were also observed in all three PC cell lines (LNCaP, DU145 and PC-3) (Fig. 1).

Immunoreactivity of ERRα in benign and malignant prostate tissues

Table I shows a summary of ERRα immunoreactivities in surgically obtained human prostate tissues. Strong immunoreactivity of

TABLE I – EXPRESSION OF ESTROGEN RELATED RECEPTOR α (ERRα) PROTEIN IN HUMAN PROSTATE (N = 106)

	Immunoreactive (IR) score[1] (%)										
	0	2	3	4	5	6	7	8	Mean ± S.D.	p-value	
Benign (n = 99)	52 (52.5)	3 (3)	10 (10.1)	23 (23.2)	8 (8.1)	3 (3)	0	0	1.8 ± 2.1		<0.0001
Malignant (n = 106)											
Low Grade[2] (n = 63)	23 (36.5)	0	8 (12.7)	12 (19.0)	6 (9.5)	10 (15.9)	3 (4.8)	1 (1.6)	3.0 ± 2.6	0.0194	
High Grade[2] (n = 43)	10 (23.2)	0	2 (4.7)	8 (18.6)	5 (11.6)	8 (18.6)	8 (18.6)	2 (4.7)	4.3 ± 2.71		

[1]Immunoreactivity (IR) score (0 to 8) was obtained as the sum of the proportion and the intensity of immunoreactivity. Proportion (0, none; 1, <1/100; 2, 1/100 to 1/10; 3, 1/10 to 113; 4, 1/3 to 2/3; and 5, >213), Intensity (0, none; I, weak; 2, moderate; and 3, strong).–[2]Low Grade: Gleason score; 2–7, High Grade: Gleason score; 8–10.

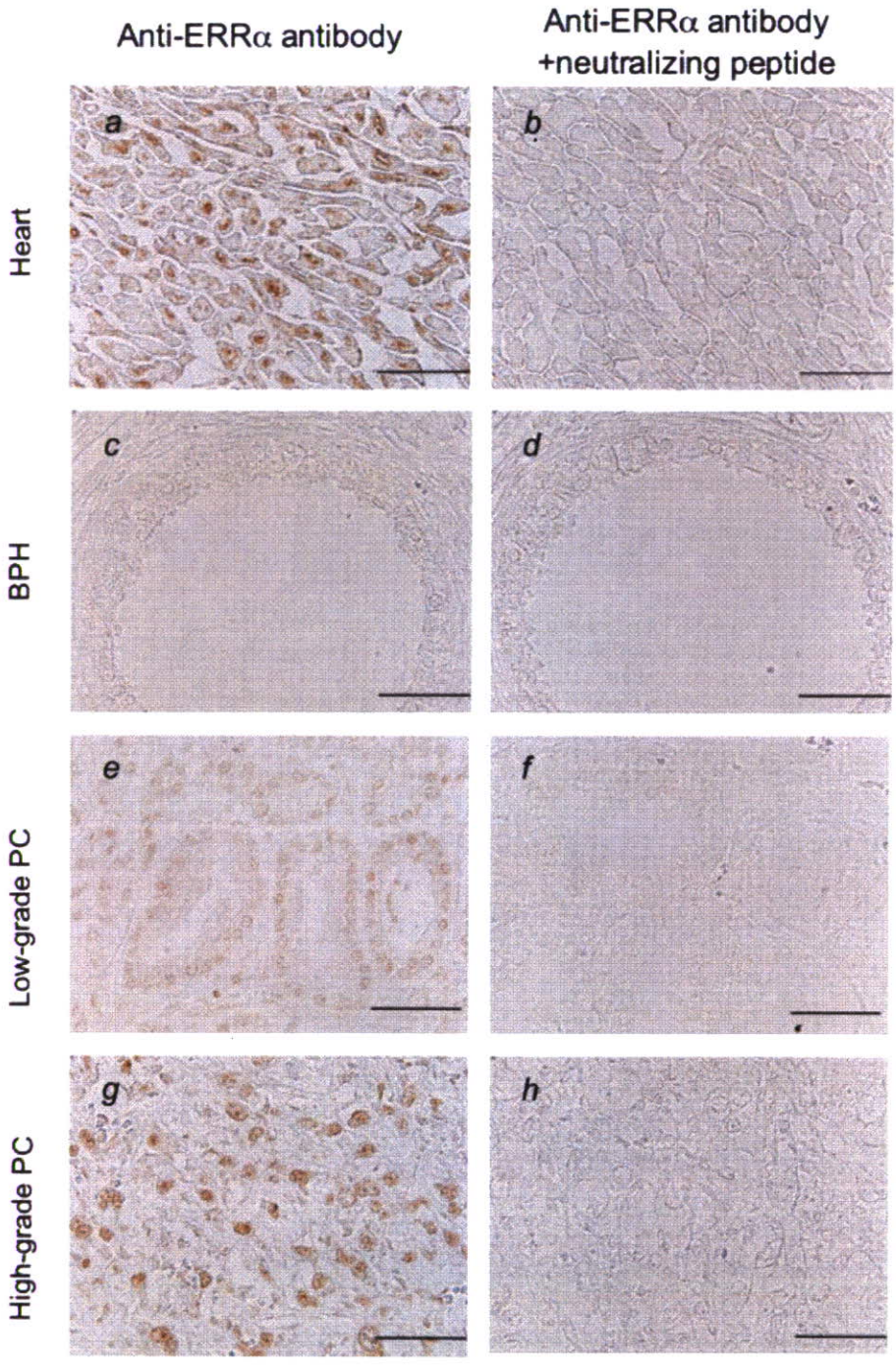

FIGURE 2 – Immunohistochemical staining (*a*, *c*, *e* and *g*) for ERRα and neutralizing peptide blocking (*b*, *d*, *f* and *h*) in human prostate and myocardium. Strong staining (IR score: 8) of ERRα was identified in the nuclei of human myocardium (*a*) Immunoreactivity was not detected in benign epithelium (*c*). Moderately increased immunoreactivity of ERRα (IR score: 6) was observed in low-grade PC (GS 6) (*e*). Extensive expression (IR score: 8) of ERRα was identified in high-grade cancer (GS 9) (*g*). Immunostaining with the ERRα antibody pre-absorbed with immunizing peptide did not identify any significant signals in all the samples examined (*b*, *d*, *f* and *h*). Original magnification; ×400, Scale bar = 50 μm.

ERRα was identified in the nuclei of human myocardium (Fig. 2*a*). Although ERRα immunoreactivity was focally detected in benign epithelium in some cases, the strong immunoreactivity (IR score: 5 or more) was rarely observed (Table I and Fig. 2*c*). No significant immunoreactivity was identified in stromal cells. In contrast, increased ERRα immunoreactivity was observed in low-grade PC (Fig. 2*e*). Extensive ERRα expression was often identified in high-grade cancer (Table I and Fig. 2*g*). Immunostaining with the ERRα antibody pre-absorbed with immunizing peptide did not identify any significant signals in all the samples examined (Figs. 2*b*,2*d*,2*f* and 2*h*). ERRα immunoreactivities were positive in 47 of 99 cases (47.5%) in benign epithelium and in 73 of 106 cancer cases (69%). The cancerous lesions showed significantly higher ERRα IR scores (3.5 ± 2.6) than 1.8 ± 2.1 of the benign foci ($p < 0.0001$). Higher-GS (8–10) cancers showed significantly higher IR score (4.3 ± 2.7), compared with the lower-GS (2–7) tumors (3.0 ± 2.6) ($p = 0.0194$)(Table I).

Clinical significance of ERRα expression in human PC

Since most of benign foci showed <5 of IR scores for ERRα, we defined IR score 5 as a cutoff for strong immunoreactivity of ERRα. Table II shows correlation of ERRα expression and clinicopathological characteristics. Cases with high serum PSA level showed a trend of strong expression of ERRα, although it did not reach statistical significance ($p = 0.07$). GS correlated with the status of ERRα expression. ERRα expression in higher-GS cancer

(8–10) was significantly higher than that in lower GS (2–7) cancer ($p = 0.0135$).

Figure 3 demonstrates a cancer-specific survival curve prepared by the Kaplan-Meier method. Eleven (10%) cases died of PC during the follow-up period. Cancer-specific survival of patients with higher ERRα expression (IR score ≥5) was significantly worse than cases with lower expression (IR score < 5) ($p = 0.0055$). Table III indicates the results of univariate and multivariate proportional analyses of cancer-specific survival with status of ERRα expression and clinicopathological parameters. ERRα expression, GS and pathological stages were significant prognostic predictors in univariable analysis ($p = 0.0141$, 0.0123 and 0.0352, respectively). Multivariate analysis showed that ERRα expression and GS are independent predictors ($p = 0.0367$ and 0.0264, respectively) among 4 parameters.

TABLE II – RELATIONSHIP OF ERRα EXPRESSION WITH CLINICOPATHOLOGICAL FINDINGS IN HUMAN PROSTATIC CANCER ($N = 106$)

	ERRα immunoreactivity[1]		*p*-value
	Weak ($n = 62$)	Strong ($n = 44$)	
Age	66.1 ± 5.8	67.4 ± 6.0	0.28
Serum PSA (ng/dl)	13.6 ± 13.0	20.5 ± 25.0	0.07
Gleason score			
2–7	43 (69.4)	20 (30.6)	0.0135
8–10	19 (44.2)	24 (55.8)	
Pathological Stage			
B, C	56 (60.9)	36 (39.1)	0.2
DI	6 (42.9)	8 (57.1)	

[1]Immunoreactivity (IR) score (0–8) was obtained as the sum of the proportion and the intensity of immunoreactivity. Proportion (0, none; 1, <1/100; 2, 1/100 to 1/10; 3, 1/10 to 1/3; 4, 1/3 to 2/3; and 5, >2/3), Intensity (0, none; 1, weak; 2, moderate; and 3, strong).IR score 0–4 and 5–8 were defined as weak and strong immunoreactivity, respectively.

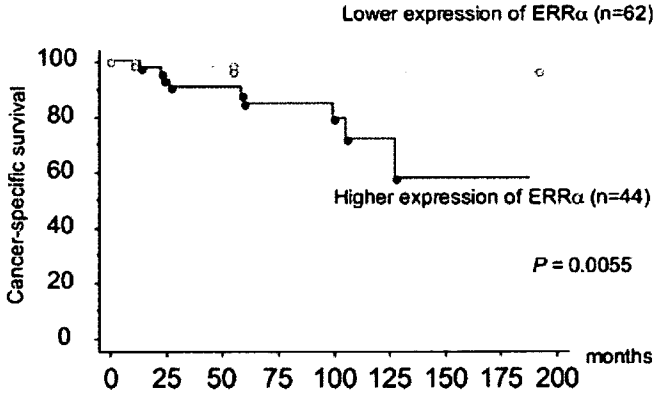

FIGURE 3 – Cancer-specific survival in 106 patients with PC according to the immunoreactivity of ERRα. Cancer-specific survival of patients with higher ERRα expression (IR score ≥ 5) was significantly worse than that of lower expression (IR score < 5) cases ($p = 0.0055$).

Discussion

Androgen deprivation and estrogen therapy have been the standard treatment for PC.[3,25,26] The growth-inhibitory effects of endocrine therapies are associated with the status of steroid receptors, such as the androgen receptor (AR) and estrogen receptor (ER).[25,26] The emergence of techniques to clone the orphan nuclear receptors in the 1980s prompted to investigate physiological functions of the orphan nuclear receptors in the targeted organs.[12,13] Among the orphan nuclear receptors, ERRα, β and γ, the three closely related members of the ERR family, all have functional links with the activities of the ERs. Two findings suggest that ERRα modulates the actions of the ERs. Firstly, ERRα shares a significant homology to ERα at the DNA-binding domain (DBD). Secondly, ERRα recognizes the ERE.[14,21,22,27,28] The ERRα gene is located on the long arm of chromosome 11.[29] Human ERRα was isolated from kidney and heart cDNA libraries by screening with an ERα-DBD cDNA probe.[11] ERRα mRNA was highly expressed in the heart and skeletal muscle and to a lesser degree in the kidney, pancreas, small intestine and colon.[29] Several investigations have implicated ERRα in the development in human breast cancer and colorectal cancer.[19,20,30] Further, ERRα mRNA has recently been detected in PC cell lines and human prostate tissues.[22] The present study is the first to reveal that ERRα expression is significantly higher in higher-GS cancer than in lower-GS cancer. These findings suggest that ERRα is involved in the normal and neoplastic growth of human prostate tissue.

Elevated ERRα expression has been identified as a poor prognostic factor in human breast cancer,[19,20] and has been reported to be correlated with higher histological grade and TNM stage of colorectal cancer.[30] However, there are conflicting data as to the ERRα expression in human prostate tissues. We found increased ERRα expression in PC, compared with that in benign epithelium. The previous study summarized the data and concluded that ERR proteins were detected as nuclear proteins in epithelial cells, whereas their expression became reduced in neoplastic prostate cells.[22] However, close interpretation of the results may suggest that these findings are more prominent in ERRβ expression, whereas ERRα rather expressed variably in PC on both the cell lines and human tissues. A figure of immunohistochemical analysis in the previous study demonstrated heterogeneous stain of ERRα in a low Gleason grade cancer, as the legend indicated.[22] Although the previous study did not identify number of cases examined with immunohistochemistry, we believed that our results obtained from 106 surgically resected prostate samples clearly demonstrate ERRα expression status in human prostate tissues and its potential significance in the cancer development. Of course, further investigations are warranted, and may let us gain better understanding on this interesting matter.

The present study suggests that ERRα participates in the regulation of PC besides ERs (α, β and βcx). How do these receptors correlate with the development of PC? We make two possible hypotheses. One is a functional cross-talk between ERRα and ERs in endocrine cancers in which ER exists. The binding of ERRα to several functional EREs has prompted speculation that ERRα can modify the ER function by either forming ER-ERRα heterodimer, by competing with ER for binding to ERE, or ste-

TABLE III – UNIVARIATE AND INULTIVARIATE PROPORTIONAL HAZARD ANALYSES OF CANCER-SPECIFIC SURVIVAL ($N = 106$)

Variable	Univariate			Multivariate		
	Hazard ratio	95% index	*p*-value	Hazard ratio	95% index	*p*-value
PSA (>10 vs. ≤10)	0.79	0.23–2.8	0.73	0.47	0.13–1.76	0.26
Gleason score (High vs. Low)[1]	2.63	1.77–108.4	0.0123	11.3	1.33–95.7	0.0264
Pathological stage (DI vs. B, C)	3.77	1.01–12.9	0.0352	1.37	0.36–5.26	0.64
ERRα (Strong vs Weak)[2]	6.84	1.47–31.8	0.0141	5.24	1.11–25.7	0.0367

[1]High Gleason score: 8–10, low: 2–7.–[2]IR score 0–4 and 5–8 were defined as weak and strong immunoreactivity, respectively.

roid receptor co-activators (SRCs).[12–14] Far-Western analysis[14] and glutathione S-transferase pull-down assays have demonstrated direct interactions between ERα and ERRα.[31] Another hypothesis is that these ERs and ERRα receptors act independently. ERα and ERRα separately modulate pS2 expression in human breast cancer.[20] As we previously assessed the expression of ERs (α/ β/ βcx) in fifty patients with PC and showed their clinical significance,[2] we estimated the correlation of ERRα with ERs (α/ β/ βcx) in overlapping fifty cases. Subsequently, no significant correlations among them were identified (R^2: 0.004 for ERα vs. ERRα, R^2: 0.006 for ERβ vs. ERRα and R^2: 0.241 for ERβcx vs. ERRα). Interestingly, similar findings were reported in breast cancer,[20] and it was suggested that ERRα might modulate the activity of estrogen responsive genes, independently of ERs. Therefore, estrogen-signaling pathway via ERs (α, β and βcx), and ERRα is so complicated that we can not reach a conclusion on the basis of current findings.

Although several investigations proved that ERRα activate a variety of estrogen target genes such as pS2, aromatase and osteopontin (OPN) and play important roles in some target organs,[13] the mechanism of ERRα in PC development remains unclear at this time. For example, ERRα regulates the expression of pS2, which increase breast cancer growth.[15,20] ERRα also activates aromatase in breast, HepG2 and bone cells.[15] Aromatase, which converts androgens to estrogens, stimulates the growth of breast cancer.[32] Recent studies focus on the surveillance about anti-aromatase effects on breast cancer.[32] Aromatase is also well known to have an important role in endocrine metabolism at the prostate. Interestingly aromatase was expressed and active in LNCaP, PC-3 and DU145 cells, whereas benign prostate epithelial cells showed no expression or activity.[33] It is not demystified how over expression of aromatase in PC correlate with PC development similar to that in breast cancer[32] because estrogens are generally considered to have protective effects on PC progressions. The local synthesis of estrogens via aromatase enzyme might contribute to the estrogen-signaling pathway through ERs in PC. In addition, OPN participates in prostate biology. For instance, elevated OPN expression is found in PC both the cell lines and human tissues.[34] Increased expression of OPN is associated with Gleason score and poor cancer-specific survival.[34] These findings suggest that further investigations are needed to verify whether the ERRα-mediated effects on PC correlate with the activation of estrogen responsive genes.

Selective estrogen receptor modulators (SERMs) are synthetic estrogen ligands that can exhibit either estrogenic or anti-estrogenic effects depending on tissue types.[35] SERMs such as tamoxifene (TAM), 4-Hydroxytamoxifen (4-OHT) and raloxifene can induce apoptosis in PC cell lines such as PC-3, DU145 and LNCaP.[36–39] Toremifene treatment significantly reduces the incidence of PC in the transgenic adenocarcinoma of mouse prostate (TRAMP) mice.[40] Toremifene also reduces the incidence of PC in high-grade intraepithelial neoplasia (PIN) patients.[41] It may be that the anti-proliferate effects of SERMs on PC are mediated via ERs due to their positive expression in the prostate. Diethylstilbestrol (DES), an agent widely used for the treatment of advanced PC, represses the molecular activities of ERRα such as reporter gene trans-activation and interaction with co-activator fragments.[42] Thus, the SERMs might inhibit PC by modulating the estrogen-signaling pathway via ERRs besides the ERs. The prognostic value of enhanced ERRα expression as an independent predictor of PC suggests that an ERRα antagonist capable of specifically blocking ERRα activity may prove useful as a therapeutic agent against PC.

References

1. Huggins C, Hodges CV. Studies on prostatic cancer. I. The effect of castration, of estrogen and androgen injection on serum phosphatases in metastatic carcinoma of the prostate. CA Cancer J Clin 1972;22: 232–40.
2. Fujimura T, Takahashi S, Urano T, Ogawa S, Ouchi Y, Kitamura T, Muramatsu M, Inoue S. Differential expression of estrogen receptor β (ERβ) and its C-terminal truncated splice variant ERβx as prognostic predictors in human prostatic cancer. Biochem Biophys Res Commun 2001;289:692–9.
3. Ho SM. Estrogens and anti-estrogens: key mediators of prostate carcinogenesis and new therapeutic candidates. J Cell Biochem 2004;91: 491–503.
4. Kirschenbaum A, Ren M, Erenburg I, Schachter B, Levine AC. Estrogen receptor messenger RNA expression in human benign prostatic hyperplasia: detection, localization and modulation with a long-acting gonadotropin-releasing hormone agonist. J Androl 1994;15:528–33.
5. Lau KM, LaSpina M, Long J, Ho SM. Expression of estrogen receptor (ER)-α and ER-β in normal and malignant prostatic epithelial cells: regulation by methylation and involvement in growth regulation. Cancer Res 2000;60:3175–82.
6. Ehara H, Koji T, Deguchi T, Yoshii A, Nakano M, Nakane PK, Kawada Y. Expression of estrogen receptor in diseased human prostate assessed by non-radioactive in situ hybridization and immunohistochemistry. Prostate 1995;27:304–13.
7. Pasquali D, Staibano S, Prezioso D, Franco R, Esposito D, Notaro A, De Rosa G, Bellastella A, Sinisi AA. Estrogen receptor β expression in human prostate tissue. Mol Cell Endocrinol 2001;178:47–50.
8. Horvath LG, Henshall SM, Lee CS, Head DR, Quinn DI, Makela S, Delprado W, Golovsky D, Brenner PC, O'Neill G, Kooner R, Stricker PD, et al. Frequent loss of estrogen receptor-β expression in prostate cancer. Cancer Res 2001;61:5331–5.
9. Pasquali D, Rossi V, Esposito D, Abbondanza C, Puca GA, Bellastella A, Sinisi AA. Loss of estrogen receptor β expression in malignant human prostate cells in primary cultures and in prostate cancer tissues. J Clin Endocrinol Metab 2001;86:2051–5.
10. Latil A, Bieche I, Vidaud D, Lidereau R, Berthon P, Cussenot O, Vidaud M. Evaluation of androgen, estrogen (ER α and ER β), and progesterone receptor expression in human prostate cancer by real-time quantitative reverse transcription-polymerase chain reaction assays. Cancer Res 2001;61:1919–26.
11. Giguere V, Yang N, Segui P, Evans RM. Identification of a new class of steroid hormone receptors. Nature 1988;331:91–4.
12. Horard B, Vanacker JM. Estrogen receptor-related receptors: orphan receptors desperately seeking a ligand. J Mol Endocrinol 2003;31:349–57.
13. Giguere V. To ERR in the estrogen pathway. Trends Endocrinol Metab 2002;13:220–5.
14. Yang N, Shigeta H, Shi H, Teng CT. Estrogen-related receptor, hERR1, modulates estrogen receptor-mediated response of human lactoferrin gene promoter. J Biol Chem 1996;271:5795–804.
15. Bonnelye E, Aubin JE. Estrogen receptor-related receptor α: a mediator of estrogen response in bone. J Clin Endocrinol Metab 2005;90: 3115–21.
16. Bonnelye E, Vanacker JM, Spruyt N, Alric S, Fournier B, Desbiens X, Laudet V. Expression of the estrogen-related receptor 1 (ERR-1) orphan receptor during mouse development. Mech Dev 1997;65:71–85.
17. Luo J, Sladek R, Carrier J, Bader JA, Richard D, Giguere V. Reduced fat mass in mice lacking orphan nuclear receptor estrogen-related receptor α. Mol Cell Biol 2003;23:7947–56.
18. Vega RB, Kelly DP. A role for estrogen-related receptor α in the control of mitochondrial fatty acid β-oxidation during brown adipocyte differentiation. J Biol Chem 1997;272:31693–9.
19. Ariazi EA, Clark GM, Mertz JE. Estrogen-related receptor α and estrogen-related receptor γ associate with unfavorable and favorable biomarkers, respectively, in human breast cancer. Cancer Res 2002;62: 6510–18.
20. Suzuki T, Miki Y, Moriya T, Shimada N, Ishida T, Hirakawa H, Ohuchi N, Sasano H. Estrogen-related receptor α in human breast carcinoma as a potent prognostic factor. Cancer Res 2004;64:4670–6.
21. Kraus RJ, Ariazi EA, Farrell ML, Mertz JE. Estrogen-related receptor α1 actively antagonizes estrogen receptor-regulated transcription in MCF-7 mammary cells. J Biol Chem 2002;277:24826–34.
22. Cheung CP, Yu S, Wong KB, Chan LW, Lai FM, Wang X, Suetsugi M, Chen S, Chan FL. Expression and functional study of estrogen receptor-related receptors in human prostatic cells and tissues. J Clin Endocrinol Metab 2005;90:1830–44.
23. Urano T, Takahashi S, Suzuki T, Fujimura T, Fujita M, Kumagai J, Horie-Inoue K, Sasano H, Kitamura T, Ouchi Y, Inoue S. 14-3-3sigma is down-regulated in human prostate cancer. Biochem Biophys Res Commun 2004;319:795–800.

24. Allred DC, Clark GM, Elledge R, Fuqua SA, Brown RW, Chamness GC, Osborne CK, McGuire WL. Association of p53 protein expression with tumor cell proliferation rate and clinical outcome in node-negative breast cancer. J Natl Cancer Inst 1993;85:200–6.
25. Culig Z, Steiner H, Bartsch G, Hobisch A. Mechanisms of endocrine therapy-responsive and -unresponsive prostate tumours. Endocr Relat Cancer 2005;12:229–44.
26. Harkonen PL, Makela SI. Role of estrogens in development of prostate cancer. J Steroid Biochem Mol Biol 2004;92:297–305.
27. Vanacker JM, Bonnelye E, Chopin-Delannoy S, Delmarre C, Cavailles V, Laudet V. Transcriptional activities of the orphan nuclear receptor ERR α (estrogen receptor-related receptor-α). Mol Endocrinol 1999;13:764–73.
28. Zhang Z, Teng CT. Estrogen receptor α and estrogen receptor-related receptor α1 compete for binding and coactivator. Mol Cell Endocrinol 2001;172:223–33.
29. Shi H, Shigeta H, Yang N, Fu K, O'Brian G, Teng CT. Human estrogen receptor-like 1 (*ESRL1*) gene: genomic organization, chromosomal localization, and promoter characterization. Genomics 1997;44:52–60.
30. Cavallini A, Notarnicola M, Giannini R, Montemurro S, Lorusso D, Visconti A, Minervini F, Caruso MG. Oestrogen receptor-related receptor α (ERRα) and oestrogen receptors (ERα and ERβ) exhibit different gene expression in human colorectal tumour progression. Eur J Cancer 2005;41:1487–94.
31. Johnston SD, Liu X, Zuo F, Eisenbraun TL, Wiley SR, Kraus RJ, Mertz JE. Estrogen-related receptor β1 functionally binds as a monomer to extended half-site sequences including ones contained within estrogen-response elements. Mol Endocrinol 1997;11:342–52.
32. Carpenter R, Miller WR. Role of aromatase inhibitors in breast cancer. Br J Cancer 2005;93(Suppl 1):S1–S5.
33. Ellem SJ, Schmitt JF, Pedersen JS, Frydenberg M, Risbridger GP. Local aromatase expression in human prostate is altered in malignancy. J Clin Endocrinol Metab 2004;89:2434–41.
34. Forootan SS, Foster CS, Aachi VR, Adamson J, Smith PH, Lin K, Ke Y. Prognostic significance of osteopontin expression in human prostate cancer. Int J Cancer 2006;118:2255–61.
35. Lonard DM, Smith CL. Molecular perspectives on selective estrogen receptor modulators (SERMs): progress in understanding their tissue-specific agonist and antagonist actions. Steroids 2002;67:15–24.
36. Suetsugi M, Su L, Karlsberg K, Yuan YC, Chen S. Flavone and isoflavone phytoestrogens are agonists of estrogen-related receptors. Mol Cancer Res 2003;1:981–91.
37. Kim IY, Seong do H, Kim BC, Lee DK, Remaley AT, Leach F, Morton RA, Kim SJ. Raloxifene, a selective estrogen receptor modulator, induces apoptosis in androgen-responsive human prostate cancer cell line LNCaP through an androgen-independent pathway. Cancer Res 2002;62:3649–53.
38. El Etreby MF, Liang Y, Lewis RW. Induction of apoptosis by mifepristone and tamoxifen in human LNCaP prostate cancer cells in culture. Prostate 2000;43:31–42.
39. Kim IY, Kim BC, Seong do H, Lee DK, Seo JM, Hong YJ, Kim HT, Morton RA, Kim SJ. Raloxifene, a mixed estrogen agonist/antagonist, induces apoptosis in androgen-independent human prostate cancer cell lines. Cancer Res 2002;62:5365–9.
40. Raghow S, Hooshdaran MZ, Katiyar S, Steiner MS. Toremifene prevents prostate cancer in the transgenic adenocarcinoma of mouse prostate model. Cancer Res 2002;62:1370–6.
41. Steiner MS, Pound CR. Phase IIA clinical trial to test the efficacy and safety of Toremifene in men with high-grade prostatic intraepithelial neoplasia. Clin Prostate Cancer 2003;2:24–31.
42. Tremblay GB, Kunath T, Bergeron D, Lapointe L, Champigny C, Bader JA, Rossant J, Giguere V. Diethylstilbestrol regulates trophoblast stem cell differentiation as a ligand of orphan nuclear receptor ERR β. Genes Dev 2001;15:833–8.

Available online at www.sciencedirect.com
ScienceDirect
Biochemical and Biophysical Research Communications 358 (2007) 813–818
BBRC
www.elsevier.com/locate/ybbrc

Estrogen-related receptor α modulates the expression of adipogenesis-related genes during adipocyte differentiation

Nobuhiro Ijichi [a], Kazuhiro Ikeda [a], Kuniko Horie-Inoue [a], Ken Yagi [b], Yasushi Okazaki [b], Satoshi Inoue [a,c,*]

[a] *Division of Gene Regulation and Signal Transduction, Research Center for Genomic Medicine, Saitama Medical University, Saitama, Japan*
[b] *Division of Functional Genomics and Systems Medicine, Research Center for Genomic Medicine, Saitama Medical University, Saitama, Japan*
[c] *Department of Geriatric Medicine, Graduate School of Medicine, The University of Tokyo, 7-3-1 Hongo, Bunkyo-ku, Tokyo 113-8655, Japan*

Received 27 April 2007
Available online 11 May 2007

Abstract

Estrogen-related receptor α (ERRα) is an orphan nuclear receptor that regulates cellular energy metabolism by modulating gene expression involved in fatty acid oxidation and mitochondrial biogenesis in brown adipose tissue. However, the physiological role of ERRα in adipogenesis and white adipose tissue development has not been well studied. Here, we show that ERRα and ERRα-related transcriptional coactivators, peroxisome proliferator-activated receptor γ (PPARγ) coactivator-1α (PGC-1α) and PGC-1β, can be up-regulated in 3T3-L1 preadipocytes at mRNA levels under the adipogenic differentiation condition including the inducer of cAMP, glucocorticoid, and insulin. Gene knockdown by ERRα-specific siRNA results in mRNA down-regulation of fatty acid binding protein 4, PPARγ, and PGC-1α in 3T3-L1 cells in the adipogenesis medium. ERRα and PGC-1β mRNA expression can be also up-regulated in another preadipocyte lineage DFAT-D1 cells and a pluripotent mesenchymal cell line C3H10T1/2 under the differentiation condition. Furthermore, stable expression of ERRα in 3T3-L1 cells up-regulates adipogenic marker genes and promotes triglyceride accumulation during 3T3-L1 differentiation. These results suggest that ERRα may play a critical role in adipocyte differentiation by modulating the expression of various adipogenesis-related genes.

Keywords: Estrogen-related receptor α (ERRα); Preadipocytes; 3T3-L1; Pluripotent mesenchymal cells; Adipocyte differentiation

Obesity is a significant risk factor for various metabolic diseases [1], as it has been recently shown that the hyperplasic adipose tissue itself alters systemic homeostasis [2]. The study for the mechanism of adipogenesis is important to understand the pathophysiology of obesity.

Estrogen-related receptors (ERRs) are orphan nuclear receptors that may regulate transcription of metabolic genes [3,4]. Among them, ERRα and ERRγ are particularly expressed in mitochondria-rich tissues [5,6], and ERRα stimulates gene expression associated with mitochondrial biogenesis and energy production [6]. ERRα-deficient mice show the reduction of fat mass and the resistance to high-fat diet-induced obesity [7], indicating that ERRα can participate in the development of white adipose tissue. The ERR coactivator peroxisome proliferator-activated receptor γ (PPARγ) coactivator-1α and β (PGC-1α and PGC-1β) are also considered as key regulators in the energy production pathways and may play a role in the regulation of mitochondrial status and functions [8–10]. Besides these previous findings, the contribution of ERRs to adipogenesis remains to be investigated.

To understand the functional roles of ERRs on adipogenesis, we investigated the expression of ERRs and adipogenic factors in 3T3-L1 and DFAT-D1 preadipocytes and C3H10T1/2 pluripotent mesenchymal cells [11,12] under

* Corresponding author. Address: Department of Geriatric Medicine, Graduate School of Medicine, The University of Tokyo, 7-3-1 Hongo, Bunkyo-ku, Tokyo 113-8655, Japan. Fax: +81 42 985 7209.
E-mail address: INOUE-GER@h.u-tokyo.ac.jp (S. Inoue).

0006-291X/$ - see front matter © 2007 Elsevier Inc. All rights reserved.
doi:10.1016/j.bbrc.2007.04.209

the adipogenic condition. We showed that ERRα mRNA was up-regulated in these cells during adipogenesis. Gene knockdown of ERRα repressed the induction of adipogenesis-related genes in 3T3-L1 cells during differentiation. Moreover, stable expression of ERRα in 3T3-L1 cells elevates the expression levels of adipogenic marker genes and promotes triglyceride accumulation during differentiation. The present study suggests that ERRα is one of the critical regulators in the signal transduction of adipogenesis.

Materials and methods

Cell culture and adipocyte differentiation. 3T3-L1 and C3H10T1/2 cells were obtained from American Type Culture Collection (Manassas, VA). DFAT-D1 cells were established from mature adipocytes of adult ddY mouse [12]. For adipogenic induction, cells (2 days after confluence) were cultured in the differentiation medium, DMEM containing 10% FBS together with the mixture of 0.5 mM isobutylmethylxanthine (IBMX, Sigma), 1 μM dexamethasone (Dex, Sigma) and 10 μg/ml bovine insulin (Sigma) (MDI mixture). On day 2 after the induction, cells were cultured in the post-differentiation medium, DMEM containing 10% FBS and 10 μg/ml insulin, and the medium was changed every 2 days (DFAT-D1) or 3 days (3T3-L1 and C3H10T1/2).

Oil-Red-O staining. Lipid accumulation was evaluated by staining with Oil-Red-O for 1 h as described previously [12].

Quantitative RT-PCR (qPCR). qPCR was performed as described previously [13]. The sequences of PCR primers are described in Table 1. The experiments were independently repeated at least three times, each performed in triplicate.

siRNA transfection. Synthetic small interfering RNA (siRNA) duplexes against mouse ERRα (ESRRA-NM_007953) and the luciferase reporter plasmid pGL2 (Luciferase GL2 Duplex) were purchased from Dharmacon (Lafayette, CO). During adipogenic induction, 3T3-L1 cells were transfected with 50 nM siRNA using Lipofectamine 2000 (Invitrogen) three times at days 0, 2, and 5.

Plasmid construction. Human ERRα cDNA (hERRα amino acids 2-475) was cloned from human brain cDNA (Clontech) by RT-PCR using the following primers: forward, 5′-CCTGAATTCTCCAGCCAGGTG GTGGGCATT-3′; reverse, 5′-ACTGAATTCTCAGTCCATCATGGC CTCGA-3′. The PCR product was N-terminally tagged with FLAG and cloned into blunted EcoRI sites of pCXN2 [14] (pCXN2-FLAG-hERRα). The construction of the plasmid was confirmed by sequencing.

Generation of stable cell lines and Western blotting. 3T3-L1 cells were transfected with pCXN2-FLAG-hERRα or empty pCXN2 plasmid and neo-resistant clones were isolated by G418 (0.8 mg/ml). hERRα mRNA expression was verified by qPCR using following primers: forward, 5′-GACTACAAGGACGATGATGACAAG-3′; reverse, 5′-CTCTGT CTCCGAGGAACCCTTT-3′.

For Western blotting, whole cell lysates were resolved by 10% denaturing SDS–PAGE and the blotted membrane (Immobilon-P Transfer Membrane, Millipore) was incubated with anti-FLAG M2 (Sigma).

Results

Up-regulation of ERRα mRNA by adipogenic induction in 3T3-L1 preadipocytes

Mouse 3T3-L1 preadipocytes have been used as a model for the adipogenesis study. 3T3-L1 cells exhibit the phenotype of adipocyte differentiation after 4-6 days of confluent culture treated with the standard adipogenic cocktail comprised of IBMX, Dex and insulin (MDI mixture) [15,16]. Using this experimental model, we investigated the expression of adipogenesis-related genes by qPCR. Oil-Red-O staining showed that triglyceride accumulation was initiated at day 2 after adipogenic induction in 3T3 cells (Fig. 1A). Consistent with the result of Oil-Red-O staining, mRNA expression of adipocyte differentiation markers aP2 and PPARγ was time-dependently elevated in 3T3-L1 cells following adipogenic induction (Fig. 1B and C). In contrast, mRNA level of uncoupling protein 1 (UCP1), which is abundantly expressed in brown adipose tissue (BAT) and known to function in adaptive thermogenesis, was transiently up-regulated by ~12-fold at day 2 after the induction (Fig. 1D). We also investigated the mRNA expression of nuclear receptor coactivators PGC-1α and PGC-1β following adipogenic stimulation. Both genes were eventually up-regulated at day 8, but the mRNA elevation of PGC-1β was observed earlier following the differentiation condition in comparison to the late induction of PGC-1α (Fig. 1E and F).

Next, we examined the mRNA expression of ERRs in 3T3-L1 preadipocytes in the adipogenesis condition. ERRα mRNA level was time-dependently up-regulated following the induction (Fig. 2A). On the contrary, ERRβ and ERRγ mRNA levels were decreased in first 5 days after the stimulation and returned to their initial levels at day 8 (Fig. 2B and C). Notably, among the three ERR subtypes, the absolute mRNA amount of ERRα was largest in 3T3-L1 preadipocytes (Table 2).

Table 1
Oligonucleotides used in qPCR

Gene	Accession No.	Description	qPCR primers (5′–3′)	
			Forward	Reverse
aP2	NM_024406	Fatty acid binding protein 4	gcgtggaattcgatgaaatca	cccgccatctagggttatga
PPARγ	NM_011146	Peroxisome proliferator activated receptor γ	cccgccatctagggttatga	ttccgaagaaccatccgatt
UCP1	NM_009463	Uncoupling protein 1	cgtaccaagctgtgcgatgt	aagccacaaacccttgaaaaag
ERRα	NM_007953	Estrogen-related receptor α	ggagtacgtcctgctgaaagct	cacagcctcagcatcttcaatg
ERRβ	NM_011934	Estrogen-related receptor β	cgatatccccgagggagatatc	ccagttgatgaggaacacaagct
ERRγ	NM_011935	Estrogen-related receptor γ	gaccctactgtccccgacagt	aactctcggtcagccaagtca
PGC-1α	NM_008904	PPARγ coactivator-1α	ggcacgcagccctattcat	cacggagagttaaaggaagagcaa
PGC-1β	NM_133249	PPARγ coactivator-1β	catctgggaaaagcaagtacga	cctcgaaggttaaggctgatatca

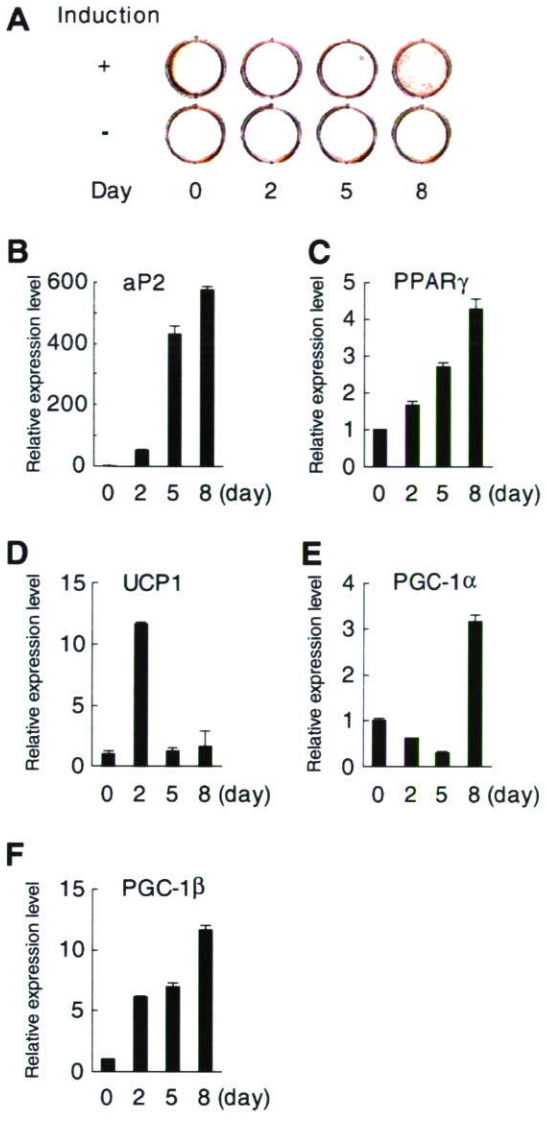

Fig. 1. Up-regulation of adipogenesis-related genes in 3T3-L1 preadipocytes under the adipogenic condition. (A) Oil-Red-O staining of 3T3-L1 cells. Two days after confluence (day 0), 3T3-L1 cells were treated with or without a MDI mixture (0.5 mM IBMX, 1 μM dexamethasone and 10 μg/ml insulin). At day 2 and 5, the medium was exchanged to DMEM/10% FBS containing 10 μg/ml insulin or vehicle. Oil-Red-O staining was performed at indicated times. (B–F) Gene expression profiles of fatty acid binding protein 4 (aP2) (B), PPARγ (C), UCP1 (D), PGC-1α (E) and PGC-1β (F) genes in 3T3-L1 cells in response to MDI treatment. mRNA expression levels of each gene were examined by qPCR and the results were shown as fold change over the expression level at day 0.

ERRα siRNA represses induction of adipocyte differentiation markers in adipogenic condition

To assess the role of ERRα on adipocyte differentiation, we investigated the effect of ERRα knockdown on the expression of adipogenesis-related genes. 3T3-L1 preadipocytes were transfected with siRNA targeted for ERRα mRNA (siERRα) in the adipogenic condition and the expression of several adipogenesis-related genes were evaluated by qPCR (Fig. 3). SiERRα reduced ERRα mRNA

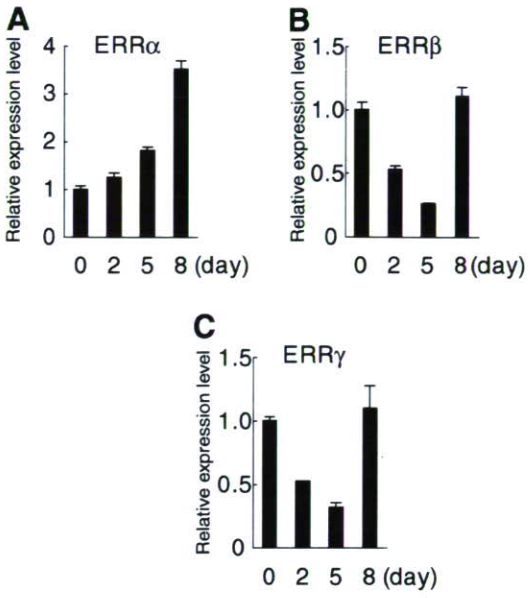

Fig. 2. Gene expression profiles of estrogen-related receptors (ERRs) in the 3T3-L1 cells under the adipocyte differentiation condition. 3T3-L1 cells were induced to differentiate as described in Fig. 1. mRNA expression levels of ERRα (A), ERRβ (B), and ERRγ (C) at indicated time points were examined by qPCR and the results were shown as fold change over the expression level at day 0.

levels by ~50% in 3T3-L1 cells compared to control siLuc, the siRNA targeted for the luciferase gene (Fig. 3A). In the adipogenic condition, siERRα attenuated the time-dependent induction of aP2 by ~50% in days 2–8 of culture compared to siLuc (Fig. 3B). Regarding PPARγ and PGC-1α mRNA, up-regulation itself was not remarkable in days 2–5 after the stimulation with siRNAs, yet siERRα repressed these mRNA induction by 35–45% at day 8 (Fig. 3C and D). These results showed that ERRα could be a modulator of the expression of adipogenesis-related genes.

Alteration of expression profile in DFAT-D1 preadipocytes and C3H10T1/2 pluripotent cells following adipogenesis

Since we found the alteration of gene expression in 3T3-L1 preadipocytes following the adipogenic induction, we next investigated whether the MDI mixture condition might also modulate gene expression in other preadipocytes or in other differentiation stages. We used mouse DFAT-D1 preadipocytes and C3H10T1/2 pluripotent cells, the former were established from ddY mouse fat and have the potential to differentiate mature adipocytes [12] whereas, the latter are pluripotent mouse embryonic fibroblasts that can differentiate into adipose, muscle, bone, or cartilage under specific conditions [17,18]. It was shown that these cell lines could differentiate into adipocytes in response to the MDI mixture [11,19]. Although not remarkable compared to 3T3-L1 cells, both DFAT-D1 and C3H10T1/2 cells exhibited intracellular lipid accumulation to some extent in the culture with the MDI mixture

Table 2
Gene expression profiles in 3T3-L1, DFAT-D1, and C3H10T1/2 cells under the adipogenic differentiation condition

Cells:	3T3-L1				DFAT-D1					C3H10T1/2			
		Fold induction[b]				Fold induction[b]					Fold induction[b]		
Gene	Day 0[a]	Day 2	Day 5	Day 8	Day 0[a]	Day 2	Day 4	Day 6	Day 8	Day 0[a]	Day 2	Day 5	Day 8
aP2	9.9E−3	50.6	430.0	574.7	2.0E−3	1.5	2.9	3.5	1.8	1.3E−3	31.9	180.2	961.4
PPARγ	4.1E−3	1.7	2.7	4.3	8.8E−4	2.8	2.2	1.9	1.5	1.3E−2	2.2	3.0	3.1
UCP1	3.4E−2	11.7	1.2	1.6	4.4E−6	2.3	1.6	2.9	1.3	1.0E−5	1.0	0.9	0.1
ERRα	2.9E−3	1.2	1.8	3.5	4.3E−5	2.6	2.2	3.1	1.6	5.0E−3	1.6	1.8	2.7
ERRβ	1.1E−4	0.5	0.3	1.1	1.1E−6	2.2	2.0	2.4	1.5	5.7E−4	1.5	0.9	0.9
ERRγ	7.9E−5	0.5	0.3	1.1	2.6E−6	2.2	2.0	3.8	1.8	6.2E−5	3.1	1.2	1.6
PGC-1α	8.6E−4	0.6	0.3	3.2	1.6E−5	0.8	1.4	1.6	0.9	8.2E−5	1.6	0.4	0.7
PGC-1β	1.1E−3	6.1	6.9	11.7	1.3E−5	2.0	5.8	8.5	3.3	2.1E−4	5.5	7.1	13.1

[a] Data represent the mean of mRNA amounts at day 0 normalized to GAPDH level.
[b] Data represent the relative mRNA level at the indicated times over day 0.

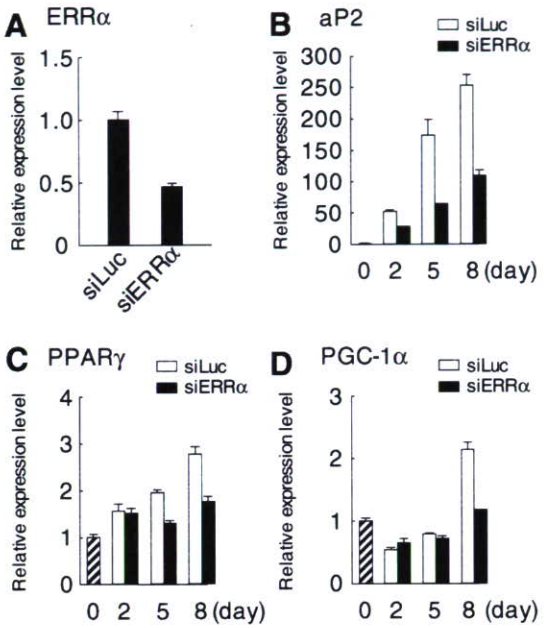

Fig. 3. Knockdown of ERRα mRNA expression leads to down-regulation of adipogenic marker genes in 3T3-L1 cells under the adipogenesis condition. (A) Reduction of ERRα expression by siRNA targeted for ERRα (siERRα). 3T3-L1 cells were transfected with 50 nM siERRα or firefly luciferase (siLuc), respectively. After 48 h, total RNA was isolated and subjected to qPCR, and the results were shown as fold change over ERRα mRNA level at day 0. (B–D) Repression of adipogenic marker genes in siERRα-treated 3T3-L1 cells under the adipogenesis condition. 3T3-L1 cells were induced to differentiate as described in Fig. 1. except for transfection of 50 nM siERRα or siLuc at day 0, 2, and 5. mRNA expression levels of the aP2 (B), PPARγ (C) and PGC-1α (D) at indicated time points were examined by qPCR and the results were shown as fold change over the expression level of each gene at day 0.

as assessed by Oil-Red-O staining (data not shown). Regarding adipogenesis-related genes, both aP2 and PPARγ mRNAs were up-regulated in DFAT-D1 and C3H10T1/2 cells under the adipogenic condition (Table 2). Especially, the fold induction of aP2 mRNA in C3H10T1/2 cells was higher than that in 3T3-L1 cells. Similar to 3T3-L1 cells, ERRα and PGC-1β mRNAs were also up-regulated in both cells following the adipogenic induction. The induction of PGC-1α was not remarkable in these cells compared to 3T3-L1 cells following the MDI stimulation, yet a slight elevation of PGC-1α mRNA was observed during the experimental period in both cells. Interestingly, ERRβ and ERRγ mRNA levels were moderately elevated in DFAT-D1 and C3H10T1/2 cells but not in 3T3-L1 cells. Cumulatively, the expression of the ERR family and its related coactivators PGC-1α and PGC-1β may be closely associated with the adipogenic signals in the process of adipocyte differentiation.

Stable expression of ERRα up-regulates adipogenic marker genes and increases triglyceride accumulation during 3T3-L1 differentiation

To further characterize the function of ERRα in adipocyte differentiation, we generated 3T3-L1 clones stably expressing FLAG-hERRα (3T3-L1-hERRα) or empty vector (3T3-L1-vector). Exogenous expression of hERRα protein was confirmed by Western blotting using anti-FLAG in 3T3-L1-hERRα clones E1 and E10, but not in 3T3-L1-vector clones C2 and C3 (Fig. 4A). mRNA expression of hERRα was also validated by qPCR using specific primers for FLAG-hERRα (Fig. 4B).

Using these 3T3-L1 clones, the alteration of adipogenesis-related gene expression was investigated by qPCR during MDI-induced differentiation as performed in Fig. 1. In general, aP2, PPARγ, and PGC-1α mRNA expression was time-dependently increased in 3T3-L1-hERRα cells during differentiation (Fig. 4B–D). In particular, E1 clones exhibited a ~8-fold and ~6-fold increase in both aP2 and PPARγ mRNA levels at day 8, respectively, compared with 3T3-L1-vector C3 cells (Fig. 4B). In regard to PGC-1α, the mRNA levels in E10 cells were also markedly increased compared with 3T3-L1-vector cells (~7-fold or ~15-fold elevation versus 3T3-L1-vector C2 or C3 cells at day 8, respectively) (Fig. 4C). Furthermore, Oil-O-Red staining revealed that the levels of triglyceride accumulation in 3T3-L1-hERRα cells were increased compared with 3T3-L1-vector cells during differentiation (Fig. 4D).

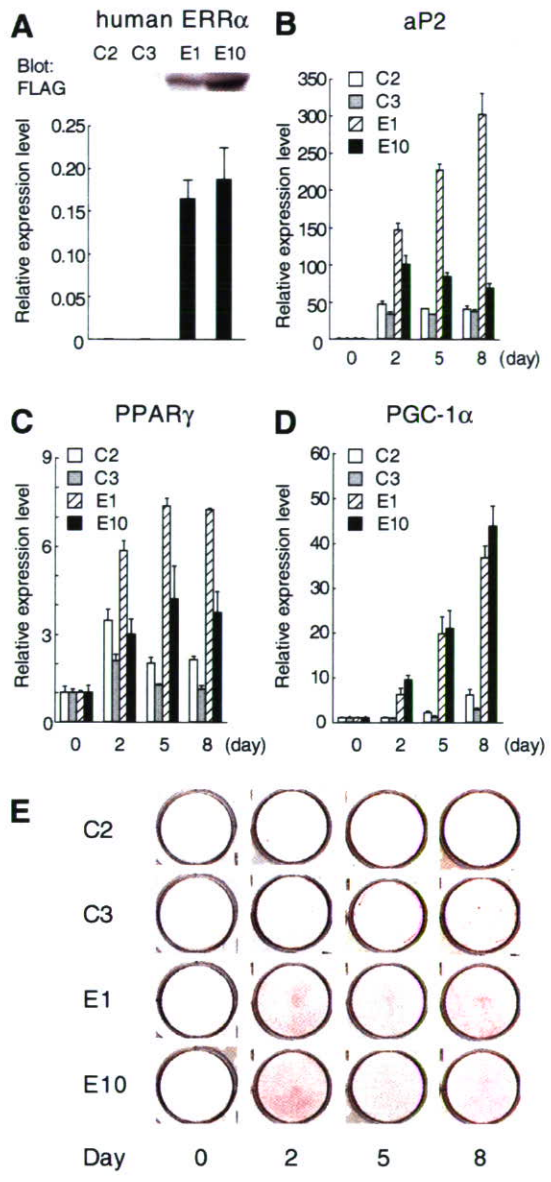

Fig. 4. Stable expression of ERRα up-regulates adipogenic marker genes and increases triglyceride accumulation during 3T3-L1 differentiation. (A) Generation of 3T3-L1 cells stably expressing FLAG-hERRα (3T3-L1-hERRα). Top panel, Expression of exogenous human ERRα protein in 3T3-L1 clones analyzed by immunoblotting using anti-FLAG (M2). C2, C3, clones expressing empty vector (3T3-L1-vector); E1, E10, 3T3-L1-hERRα. Bottom panel, Expression of exogenous human ERRα mRNA validated by qPCR. (B–D) Stable expression of ERRα up-regulates adipogenic marker genes during 3T3-L1 differentiation. 3T3-L1 clones were maintained in the differentiation medium as described in Fig. 1. mRNA levels of the aP2 (B), PPARγ (C), and PGC-1α (D) in each clone at indicated times were examined by qPCR and the results were shown as fold change over the expression level in each clone at day 0. (E) Oil-Red-O staining of 3T3-L1 clones.

Taken together, gain- and loss-of-function study for ERRα reveals that this nuclear receptor positively regulates the expression of adipogenesis-related genes as well as its coactivator PGC-1α, and functions as a promoting factor for 3T3-L1 differentiation.

Discussion

In the present study, we showed that ERRα mRNA expression was up-regulated in response to the adipogenic induction including IBMX, Dex, and insulin in 3T3-L1 and DFAT-D1 as well as C3H10T1/2 cells. Under this differentiation condition, PGC-1α and PGC-1β expression was also increased in parallel with ERRα in those cells. ERRα knockdown by the specific siRNA repressed the adipogenesis-related induction of aP2, PPARγ, and PGC-1α in 3T3-L1 cells. Furthermore, stable expression of ERRα in 3T3-L1 cells significantly up-regulated adipogenesis-related genes and increased triglyceride accumulation during differentiation. These results provide the first evidence that ERRα positively regulates the expression of adipogenesis-related genes during adipocyte differentiation.

ERRα is predominantly expressed in mitochondria-rich tissues such as brown adipose tissue and cardiac myocytes and to play a critical role in the regulation of gene expression involved in mitochondria biogenesis, oxidative phosphorylation, and β-oxidation of fatty acids [20–22]. ERRα itself is not a constitutively active receptor and no small lipophilic ligand has been identified for the receptor. Instead, PGC-1α and PGC-1β have been identified as potential protein ligands for ERR family [8,9]. PGC-1α has been originally identified as an interacting factor for PPARγ [23] and can potentially activate many nuclear receptors. Mice lacking either PGC-1α or ERRα exhibit phenotypes with being lean and resistant to high fat diet-induced obesity [7,24], suggesting that PGC-1α and ERRα function in the same signal pathway. It is also confirmed that PGC-1α mRNA expression in brown fat of ERRα knockout mice is almost half of the expression in wild-type mice [25].

PGC-1β is considered as a more ERR-specific coactivator and protein ligand that may regulate the ERR-mediated transcription [9,26,27]. PGC-1β plays a critical role particularly in energy production in brown fat. PGC-1β transgenic mice are lean, of elevated energy expenditure, and resistant to high fat diet-induced obesity [9]. Although the precise function of PGC-1β in adipogenesis remains to be studied, our results suggest that PGC-1β may also be involved in adipogenesis.

Recently, ERRα has been also shown to regulate the transcription of the nuclear receptor corepressor RIP140/NRIP1 that mediates an inhibitory feedback mechanism to control the adipogenesis-related gene expression during differentiation [28,29]. Thus, ERRα may function as a key regulator in both stimulatory and inhibitory mechanisms for adipogenesis.

ERRβ and ERRγ expression was induced in DFAT-D1 and C3H10T1/2 cells but not in 3T3-L1 cells in the present study. The difference of gene expression may be related to each cell-specific character that represents distinct stages of adipogenesis. Further study will reveal the roles of these receptors during adipogenesis.